DYNAMIC MECHANICAL ANALYSIS OF UNIRRADIATED AND GAMMA RAY RADIATED INJECTION MOLDED VIRGIN AND RECYCLED HIGH DENSITY POLYETHYLENE.

By

KING'ORI GLADYS WANGECHI
B. Ed. Sc. (Hons)

A thesis submitted in partial fulfillment of the requirements for the award of the degree of Master of Science, in the School of Pure and Applied Sciences of Kenyatta University.

School of Pure and Applied Sciences
Department of Physics

March 2007

Declaration

This thesis is my original work and has not been presented for the award of a degree in any other University or any other award.

All sources of information have particularly been acknowledged by means of references.

.....

King'ori Gladys Wangechi

We confirm that the candidate, under our supervision, carried out the work reported in this thesis.

.....

DR. A. S. MERENGA,
DEPARTMENT OF PHYSICS,
KENYATTA UNIVERSITY,
P.O. BOX 43844,
NAIROBI-00100 GPO.
KENYA.

.....

DR. C. M. MIGWI,
DEPARTMENT OF PHYSICS,
KENYATTA UNIVERSITY,
P.O. BOX 43844,
NAIROBI-00100 GPO.
KENYA.

Dedication

To my son Oscar Patrick and daughter Ann Tracy

and

my parents Joseph King'ori and Elizabeth Wanjiru

Acknowledgements

I am profoundly grateful to my research supervisors, Dr. A.S. Merenga and Dr. C. M Migwi for their relentless guidance, corrections and suggestions throughout this work. Their vast knowledge in the research area and links with the research world were tremendously invaluable. I am particularly indebted to Prof. Tole of Nairobi University who facilitated sample irradiation at Nairobi Hospital, and also to Ms. Westphal of University of Leipzig (Germany) for facilitating the DSC measurements. Thanks too to Kenyatta University Physics department for availing the DMA equipment. I am grateful to all the postgraduate students and members of the technical staff of the department of Physics, Kenyatta University for their encouragement and support during this research.

Last, but by all means supreme, I am inexpressibly thankful to the Almighty God, Who Has faithfully been by my side and my guide in the entire course of scaling the academic ladder.

ABSTRACT.

Modification in polymeric molecular structure can be brought about by either the conventional chemical means, usually involving silanes and peroxides, or by exposure to ionizing radiation, from either radioactive sources or highly accelerated electrons. In this work ionizing radiation from a radioactive source, in this case a standard ray from a Cobalt 60 source was used to irradiate injection molded samples of both recycled high density polyethylene (RHDPE) and virgin high density polyethylene (VHDPE). The samples were then studied using a Dynamic mechanical analyzer (DMA) and the Differential Scanning Calorimetry (DSC). The DMA measurements were done in a temperature range of 298 K to 355 K in the frequency range of 0.5 Hz to 13 Hz. One relaxation process was observed which follows the Vogel Fulcher Tammann (VFT) law of the temperature dependence of the mean relaxation for both VHDPE and RHDPE. The process is assigned to chain motions between the crystals. It was noted that doses of at least 12 kRad had no effect on the frequency of the relaxation process of VHDPE or RHDPE. This suggests irradiation effect on a small (local) scale. Another observation was that irradiation resulted in an increase of the loss modulus intensities, for VHDPE and a decrease in the RHDPE. For both the gamma ray radiated and unirradiated samples the intensities of the samples cut far from the injection point were higher than for samples cut near the injection point. As regards anisotropy of the samples, a comparison of the intensities of the loss modulus for samples cut parallel and those cut perpendicular to the polymer melt flow directions indicate that irradiation has a stronger influence on the samples cut perpendicular to the melt flow direction than those cut parallel. Anisotropy between the samples cut near and those cut far from the injection point was unaffected by irradiation. DSC thermograms were obtained at a heating rate of 10 K/min from 270K to 410K. From the DSC thermogram it was observed that irradiating RHDPE to a dose of up to 6 krad decreases its melting temperature, however for a dose of up to 12 krad, the melting temperature of VHDPE was insignificantly affected.

TABLE OF CONTENT

CHAPTER FOUR
Experimental technique

CHAPTER FIVE
Results and discussion.

CHAPTER 6
Conclusion and recommendations

List of figures

List of tables

List of abbreviations

Abbreviation	Name in full
AFM	Atomic force microscopy
ATR	Attenuated total reflection
B	A constant given by Cohen-Turnbul free volume theory
DMA	Dynamic mechanical analyzer
$\dot{D}_P$	Absorbed dose in medium
DSC	Differential scanning calorimetry
$\dot{D}_W$	Absorbed dose in water
E	Spring constant
E'	Storage modulus
E''	Loss modulus
ESR	Electron Spin Resonance
F_0	Is the attempt frequency of the polymer chain before it finally responds to the applied stress.
FFM	Frictional force mode
FTIR	Fourier Transform Infra Red Spectroscopy
HDPE	High density polyethylene
ip	Ion pairs
J(t)	Creep compliance
k	Boltzmann contant
LDPE	Low density polyethylene
MEMA	Morpholino ethyl methacrylate

NMR	Nuclear Magnetic Resonance
PCMC	Poly (carboxymethyl cellulose)
PE	Polyethylene
PEO	Polyethylene oxide
PP	Polypropylene
PTFE	Polytetrafluoroethylene
PVA	Poly (vinyl alcohol)
PVP	Poly-N-vinylpyrrolidone
Q	Electrical power
R0A	Unirradiated recycled sample cut along the melt flow direction
R0F	Unirradiated recycled sample cut far from the injection point
R1F	Recycled sample cut far from the injection point irradiated to a dose of 6 krad
R1N	Recycled sample cut near the injection point irradiated to a dose of 6 krad
RHDPE	Recycled high density polyethylene
SEM	Scanning electron microscopy
SLS	Standard linear model
T	Absolute temperature
t	Time
T_0	Ideal temperature which is 50 ^{0}C below the calorimetric glass transition

Tg	Glass transition
T_m	Melting temperature
T_R	Temperature of reference sample
T_S	Temperature of sample
U	Energy
UHMWPE	Ultra high molecular weight polyethylene
V	Total volume
V^*	Minimum volume required for relaxation to take place
V_0	Occupied volume
V0A	Unirradiated virgin sample cut along flow direction
V0P	Unirradiated virgin sample cut perpendicular to the flow direction
V1A	Virgin sample cut along flow direction irradiated to a dose of 6 krad
V1P	Virgin sample cut perpendicular to the flow direction irradiated to a dose of 6 krad
V2A	Virgin sample cut along flow direction irradiated to a dose of 12 krad
V2F	Virgin sample cut far from the injection point irradiated to a dose of 12 krad
V2N	Virgin sample cut near the injection point irradiated to a dose of 12 krad
V2P	Virgin sample cut perpendicular to the flow direction irradiated to a dose of 12 krad
VFT	Vogel Fulcher Tamann
V_m	Mean volume of relaxing polymer segment

List of symbols

Symbol	What the symbol represents
ρ	Density
$\dot{D}$	Dose rate
$\dot{D}_p$	Absorbed dose in Polyethylene
$\dot{D}_w$	Absorbed dose in water
β	Secondary relaxation
ε	Strain
σ	Stress
η	Viscosity
τ	Relaxation time
ψ	Heating rate
λ	Past time
δ	Phase angle
ω	Angular frequency
μ_A	Average energy absorption co-efficient
ξ	A constant that lies between 0.5 and 1
α	Volume thermal expansion coefficient

CHAPTER 1

INTRODUCTION

1.1 Background to the Research Project

A great deal of materials for construction, manufacture of vehicles, aircrafts, grocery bags, ships, toys, snap on lids, battery parts, blow molded bottles, furniture and household appliances come from the plastics industry (Reyes *et al*, 2000). High density polyethylene (HDPE) is a widely used polymer due to the fact that it is available in many forms. It is cheap and has outstanding features such as, regular chain structure that leads to high degree of crystallinity and good mechanical properties, processability and chemical resistance. Polyethylene (PE) is a member of the chemical compounds known as Polylefins. It is a polymer whose repeating unit or 'mer' is the hydrocarbon ethylene (C_2H_4), the molecule formed is a long chain consisting of a carbon back bone surrounded by hydrogen atoms as shown in the figure below.

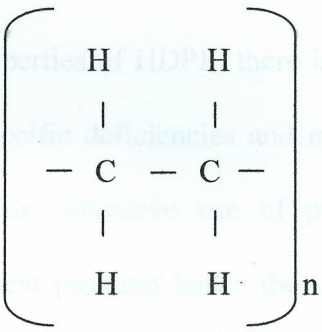

Figure 1.1. A two dimensional section of polyethylene, this chain can extend both left and right.

Polyethylene is prepared through addition polymerization of ethylene monomers, using organometallic compound as catalysts at moderate pressure (15 to 30 atm). It exists in a number of forms, depending on the production process, which include low density (branched) polyethylene (LDPE), high density (linear) polyethylene (HDPE) which is normally produced with a molecular weight in the range of 200 000 - 500 000 g/mole. Another form is the ultra high molecular weight polyethylene (UHMWPE) produced with molecular weights in the range of 3-6 million g/mol (Mark *et al*, 1984). HDPE is highly crystalline (over 90%) with a melting point in the range of 400 - 408 K (Fried, 1995), a density in the range of 0.95 – 0.97 g/cm^3. It is stiffer (modulus of 6.897×10^8 Pa) with good tensile strength and hardness, low temperature brittleness and low permeability to gases and vapors (James, 1986).

The intensive use of polymers makes it necessary to create new materials with enhanced properties while at the same time avoiding use of chemical additives prohibited in some areas such as pharmaceutical industry and medicine (Reyes *et al*, 2000). Despite the generally excellent properties of HDPE, there is still need to modify and regulate its properties to overcome specific deficiencies and make it more suitable for a particular application. Furthermore the intensive use of polymers has brought about a huge environmental and ecological problem hence the necessity to create new materials that use recycled components with enhanced properties. One way of achieving this is the use of ionizing radiation, which even at low doses causes polymers to undergo structural changes such as molecular cross linking, grafting and chain scission reactions. Polymer irradiation is the only technique that allows introduction of energy into the material to

generate change, besides, it leaves no residuals of substances required to initiate chemical cross linking that could limit its application possibilities (Reyes *et al*, 2000).

Polymeric materials are often used in situations that challenge the thresholds of their thermal capabilities, it is therefore important to understand polymeric material behavior under the influence of thermal loads. The dynamic mechanical analysis (DMA) and differential scanning calorimetry (DSC) provide such information. In addition the methods offer information that helps to compare properties of similar materials and characterize them.

The DMA is a method of monitoring property changes in materials as they are cycled through a range of temperatures. It measures changes in mechanical behavior such as modulus and damping as a function of temperature, time, frequency, stress or a combination of these parameters. As a result it helps to project the long-term time dependant behavior of polymeric materials under constant load. It therefore provides a tool for studying the mechanical properties of injection-molded materials (Sepe, 1992). DSC on the other hand measures the temperature and heat flow associated with transitions in materials as a function of time and temperature. It provides quantitative and qualitative information about physical and chemical changes that involve exothermic and endothermic processes, which in turn helps in evaluation of small transitions like those due to side chains in polymers. DSC allows accurate determination of temperatures associated with thermal events, and also reveals thermal histories imparted to thermoplastics as a result of different processing conditions. In this work DMA and DSC were used as techniques for taking measurements. The main focus was to study the

effects of radiation dose on the mechanical properties of unirradiated and gamma ray radiated injection molded virgin and recycled HDPE.

1.2 Objectives

The research work aimed at producing injection-molded samples of HDPE, and then irradiating them with gamma rays. In general, effects of gamma ray radiation on the mechanical properties of injection molded virgin and recycled HDPE were investigated. The specific objectives were to investigate the effect of gamma ray radiation on,

a) Loss and storage modulus.

b) Glass transition and melting temperatures.

c) Activation energy of the relaxation processes observed.

d) Anisotropy in the direction parallel and perpendicular to the melt flow.

e) Anisotropy near and far away from the injection point.

1.3. Rationale

Through the injection molding process, HDPE can be put into numerous uses such as, manufacture of injection molded crates, pails, tanks, toys, household appliances, furniture, caps and closures, floor coverings, and many others.

In order to optimize polymer selection and design for specific application it is necessary to elucidate the origin of physical properties in molecular structure and to control the structure by processing. The injection molding process has been found to influence the molecular dynamics in HDPE. The chain motions are closely related to the mechanical properties of the polymer. The inter-chain interactions affect the molecular

dynamics in polymeric systems. Since cross-linking and chain scission occur upon gamma irradiation (Mark *et al*, 1988), it was of interest to investigate the effect of gamma irradiation on the molecular dynamics of injection molded systems in the direction parallel and perpendicular to the melt flow as well as near and far away from the injection point. A comparison was made on the effect of gamma-irradiation on recycled HDPE.

Polymers are often used in applications that involve stresses such as in housings, gears, ropes, structures and many others. Before using them in load bearing applications we must study the effect that stress has on them. Dynamic mechanical tests provide information about viscoelastic properties, thermal transitions, and molecular relaxations. Any mechanical property may be affected by temperature and hence the need to do the tests at various temperatures.

CHAPTER 2

2.1 LITERATURE REVIEW.

Long chain polymers owe many of their properties to the structural arrangement of their molecules. These can be profoundly affected by exposure to high-energy radiations and new properties emerge often difficult to achieve by other means (Ian, 1996). Through irradiation, polymers can be modified in clearly defined ways and to a reproducible extent (Cheng and Kerluke, 2003).

Reyes *et al* studied effects of gamma ray radiation on Polypropylene (PP), and observed an increase in the Young's modulus and an abrupt decrease in the elongation at break for doses less than 5 Mrads, with cross linking effect being dominant. For doses greater than 5 Mrads chain scissions are dominant, (Reyes *et al*, 2000). Valenza and Spadaro studied the effect of gamma ray radiation on LDPE and observed an abrupt decrease in its molecular weight for doses of 1Mrad and attained stability at doses higher than 5 Mrads (Valenza and Spadaro, 1993).

Albano *et al* studied the effects of gamma rays on different polyethylenes using (Electron Spin Resonance) ESR, (Fourier Transform Infra Red Spectroscopy) FTIR and differential scanning calorimetry, they observed that chemical reactions produced during radiation as well as during the storage time are mainly cross linking, chain scission and/or branching. The percentage of each of these reactions was found to depend on the linearity of polyethylene (Albano *et al*, 2003).

Zainuddin *et al* studied the effects of gamma irradiation on solid polyethylene oxide by gel permeation chromatography and viscometry. They observed that irradiation of polyethylene oxide powder in presence of oxygen leads to the dominance of chain

scissions reactions. Upon irradiation in vacuum, crosslinkng and chain scission occur side by side and the changes in molecular weight are less pronounced in the studied dose range (up to 20 kGy). Scission dominates for doses of up to 15 kGy, while for higher doses intermolecular crosslinking gains in importance. Competition between between these processes was observed to depend on the applied dose and also by the inhomogenity of the material (molecular weight and/or possibly the crystallinity). The study also revealed that the parallel occurrence of chain scission and crosslinking leads to the broadening of the molecular weight distribution (Zainuddin *et al*, 2002).

Zhen studied the effect of chain flexibility and chain mobility on radiation crosslinking of polymers. From the results obtained they concluded that the flexibility and mobility of the chain directly influence the possibility of reactive radicals recombination. Flexible chain is easier to crosslink than rigid-chain polymer, the rigid chain polymer must be crosslinked at high temperature, as most polymers can only crosslink above their melting point (Zhen, 2001).

Maggi *et al* conducted a study of gamma radiation on two kinds of matrix tablet formulations containing polyethylene oxides (PEO) and Poly (vinyl alcohol) (PVA), as drug release modulators. The results showed that ionizing radiation does not modify significantly the dissolution trend of the PVA samples, however dissolution and morphological behavior of the PEO matrices is strongly affected by the radiation dose received. In particular the dissolution rate of the irradiated PEO tablets dramatically increases as a function of the irradiation dose and the swelling process, (which characterized the non irradiated PEO samples), was replaced by a rapid erosion process responsible for the quick dissolution of the matrices. They concluded that there was

breaking of polymeric chains (shown by EPR) as a consequence of exposure to gamma rays (Maggi *et al*, 2004).

Banerjee *et al* used the atomic force microscopy (AFM) in frictional force mode (FFM) to detect the onset of chain scission and crosslinking of gamma ray irradiated elastomer surfaces, the elastomers of concern were, ethylene-propylene-diene monomer rubber and fluorocarbon rubber. They observed that both elastomers show systematic smoothening of its surfaces, as the gamma dose rate increased. The frictional property studied using FFM of the sample surfaces show an initial increase and then a decrease as a function of dose rate. Increase in the surfaces' frictional property is attributed to the onset of chain scission, while the subsequent decrease is attributed to the onset of crosslinking of polymer chains (Banerjee *et al*, 2007).

Mansour, studied the effect of different doses of gamma irradiation on the mechanical and relaxation properties of HDPE and LDPE. He found out that HDPE is more susceptible than LDPE to the influence of radiation (Mansour, 2001).

Usanmaz *et al* studied thermal and dynamic mechanical properties of gamma ray cured poly (methyl methacrylate) used as a dental-base material. DSC and DMA analysis revealed that gamma ray curing produced a material with superior qualities in terms of producing high molecular weight homogeneous polymers with low porosity and crosslinking (Usanmaz et al, 2001).

Evora *et al* studied the ionizing radiation effects on thermal properties of recycled polyamide-6, irradiated with an electron beam of 1.5MeV. They observed that recycled polyamide-6 undergoes crosslinking upon irradiation (Evora *et al*, 2002).

The effects of ionizing radiation on piezoelectric films of poly (vinylidine flouride) have been examined. It was observed that heat shrinkage of the films is reduced by irradiation. After annealing at 153^0 C, the length of an unirradiated polymer film is less than 80% of the initial length, while as that of a film irradiated to a dose of 100 kGy is 93% of the initial length. Irradiation also increased heat stability of the films. These observations were attributed to crosslinking of poly (vinylidene fluoride) (Koizumi *et al*, 2004).

Gamma ray or electron beam irradiation at high temperature and at a small dose 3 to 5 kGy improved the Rockwell hardness and resistance to wear for polycarbonate and polysulfone. The effect for hardness was same between gamma ray and the electron beam. Main chain scission was predominant for both polymers (Seguchi *et al*, 2002).

El-Salmawi *et al* studied sorption of dye wastes by Poly (vinyl alcohol) (PVA) /poly (carboxymethyl cellulose) (PCMC) blend grafted through radiation method. Spectroscopic analysis indicated that the blend-grafted co-polymer has a high affinity for basic acid and active dyes (El-salmawi *et al*, 2003).

Nho *et al* investigated the effect of gamma ray radiation dose on the physical properties of PVA/poly-N-vinylpyrrolidone (PVP) hydrogels containing chitosan. The hydrogels were prepared by a combination of freezing, thawing and gamma ray radiation. They found that the physical properties of hydrogels such as gelation and gel strength were higher when a combination of freezing, thawing and irradiation were used than just freezing and thawing, the PVA/PVP-chitosan combination and the irradiation dose had a greater influence on swelling than the gel content (Nho *et al*, 2002).

El-Naggar *et al* studied the antimicrobial protection of cotton/polyester fabrics by gamma as well as by electron beam irradiation, and thermal treatment. They observed that treatment using electron beam irradiation provided better protection than gamma ray radiation and thermal curing (EL-Naggar *et al*, 2003). Gawish *et al* investigated radiation induced grafting of 2N –Morpholino ethyl methacrylate (MEMA). It was found that the graft yield increased with increasing pre-irradiation dose (Gawish *et al*, 1995). Mukherjee and Gupta studied the dyeing behavior of polypropylene-g-polymethacrylic acid prepared by graft co-polymerization of methacrylic acid onto Polypropylene fibers by gamma ray irradiation and found that the diffusion coefficient of the fiber showed an increase with the increase in graft content. They attributed this observation to the structural changes occurring during grafting (Mukherjee and Gupta, 1985)

Kaufman *et al* did a study to evaluate the effects of gamma ray radiation sterilization on the material properties of ultra high molecular weight polyethylene (UHMWPE). They observed that the irradiated material was harder and more resistant to creep deformation. The irradiated sample however also exhibited a higher coefficient of friction and reduced abrasive wear resistance (Kaufman *et al*, 1998). In an almost similar study, Borgstorm *et al* studied the mechanical properties of processed UHMWPE. They conducted studies on a non-sterilized compression molded block and also on the inner and surface regions of a gamma ray radiated knee implant. They also observed that compression molding caused a decrease in percent crystallinity between the resin and the block from 86.51% to 52.40%. However gamma ray radiation and further machining caused crystallinity of the material to increase to 59.58%. They also observed that there was no statistical difference between the densities, percent crystallinities or elastic moduli

of the interior and surface of the Gamma ray radiated implant. Also no discoloration due to oxidation was observed under a light microscope (20X). The results were an indication of insignificant oxidation in the implant (Borgstorm *et al*, 1998).

Besides the already described studies, radiation processing has been applied to crosslink insulation on electrical wires and cables, especially those made of polyethylene, polyvinylchloride, polyvinylidene fluoride and ethylene-tetrafluoroethylene copolymer, in order to increase the insulation's tolerance to high temperature, also radiation increases their resistance to solvents and corrosive chemicals (Cheng and Kerluke, 2003). Electron beam radiation has also been used to irradiate polytetrafluoroethylene (PTFE), which undergoes chain scissioning, making it very brittle. As a result it becomes possible to grind scrap PTFE into fine particles during recycling. Unirradiated PTFE is tough, slippery, and doughy hence impossible to grind (Cheng and Kerluke, 2003).

Despite the extensive work that has been done in this area, coupled with the extensive use of HDPE in our local industries, investigations on the dynamic mechanical analysis of gamma ray radiated injection molded virgin and recycled HDPE are sparse. This work therefore intends to provide an understanding of the effect of radiation dose on the mechanical properties of virgin and recycled HDPE.

CHAPTER 3

THEORETICAL ASPECTS OF THE DMA MEASUREMENT TECHNIQUE

3.1 Introduction

Molecular dynamics of a polymer can be studied by a number of techniques namely, dynamic mechanical analysis (DMA), differential scanning calorimetry (DSC), small angle x-ray scattering, scanning electron microscopy, among others. The main method that was used in this work is the DMA, with the DSC only being used as a supplementary method. The loss modulus curves are used to interpret the molecular dynamics of the polymer, when the polymer chain environment changes. In this case the change may be due to irradiation, variation in temperature, stress or strain. These changes affect chain movement, which in turn has a macroscopic effect on the physical characteristics such as, stiffness, ductility, brittleness and mechanical strength.

In order to understand the mechanical properties measurements and parameters involved in polymers, a brief viscoelastic theory is presented below followed by the DMA and DSC measurement technique.

3.2 Viscoelastic Theory

Polymer molecules respond to an external force in two ways. Part of the response is instantaneous and this is referred to as the elastic response. All the mechanical energy put in is recovered upon release of the external force, and thus this part is associated with energy storage. The other part is a delayed response that involves dissipation of mechanical energy into heat as in the flow of a viscous liquid (Bovey and Winslow, 1979). Viscoelasticity is a combination of the two responses.

In other words, viscoelasticity is a combination of viscosity and elasticity in varying amounts, meaning that a polymeric system does not follow a Hookean (elastic), or viscous (flow) behavior. Various models have been proposed to explain viscoelastic behavior. These include, Kelvin (or Voigt), Standard linear solid (Zener) and Maxwell-Wiechert models, among others (Sperling, 1992; Williams, 1980; Fried, 1995).

This work has adopted the Standard linear solid model, because the model provides a good qualitative description of both creep and stress relaxation behavior of polymeric materials. The responses of this model, under both creep and stress relaxation conditions will be analyzed. In this case a linear model will be considered, meaning that at any point in time, stress is directly proportional to the strain. The basic elements for all the models that explain the viscoelastic behavior are:

(a) Linear spring, which represents the elastic component.

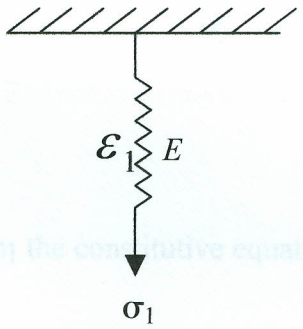

Figure 3.1; Linear spring - Elastic component

Where

E is the spring stiffness.

ε_1 is the strain due to the spring

σ_1 is the applied stress.

The constitutive equation for this element is the Hooke's law, which gives

$$\sigma_1 = E\varepsilon_1 \tag{3.1}$$

(b) Linear dashpot, which forms the viscous component

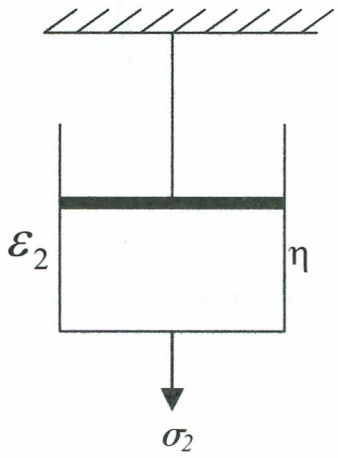

Figure 3.2; Linear dashpot - Viscous component

For a liquid with viscosity η the constitutive equation relating stress (σ_2), to strain (ε_2) is

$$\sigma_2 = \eta \frac{d\varepsilon_2}{dt} \tag{3.2}$$

The standard linear solid model combines a spring and a Kelvin element as shown in Figure 3.3.

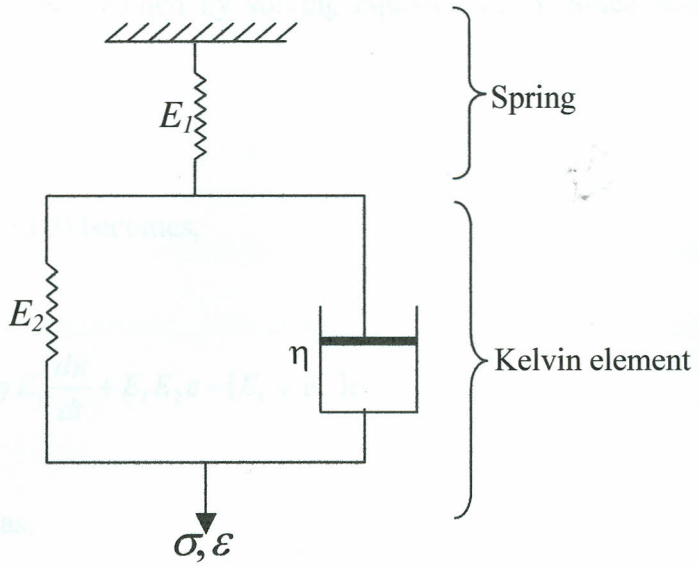

Figure 3.3; Standard Linear Model: Spring and Kelvin model in series

By considering equilibrium of stresses and compatibility of strains, the governing equation for this model is

$$\eta E_1 \dot{\varepsilon} + E_1 E_2 \varepsilon = \eta \dot{\sigma} + (E_1 + E_2)\sigma \qquad (3.3)$$

where $\dot{\varepsilon} = \frac{d\varepsilon}{dt}$ and $\dot{\sigma} = \frac{d\sigma}{dt}$, (McCrum *et al*, 1997).

This is a linear equation in stress and strain and their first derivatives. The equation can be solved by integration for conditions of creep or stress relaxation.

3.2.1 *Creep Testing*

In a creep test, a constant stress (σ_0) is instantaneously applied to the polymeric material and the resulting strain followed as a function of time. For a constant stress (σ_0),

the corresponding strain is obtained by solving equation (3.3). Since stress (σ_0) is a constant,

$\frac{d\sigma}{dt} = 0$ and equation (3.3) becomes,

$$\eta E_1 \frac{d\varepsilon}{dt} + E_1 E_2 \varepsilon = (E_1 + E_2)\sigma \tag{3.4}$$

which can be rewritten as,

$$\frac{d\varepsilon}{dt} + \frac{E_2 \varepsilon}{\eta} = (E_1 + E_2)\frac{\sigma}{\eta E_1} \tag{3.5}$$

Noting that the equation has an integrating factor, $e^{\frac{E_2 t}{\eta}}$, we obtain an expression for strain as

$$\varepsilon e^{\frac{E_2 t}{\eta}} = (E_1 + E_2)\frac{\sigma}{E_1 E_2} e^{\frac{E_2 t}{\eta}} + C \tag{3.6}$$

At $t = 0, \varepsilon = \frac{\sigma_0}{E_1}$, substituting these values in (3.6) and solving for C, we obtain an expression for strain as,

$$\varepsilon(t) = \frac{\sigma_0}{E_1} + \frac{\sigma_0}{E_2}\left[1 - \exp\left(-\frac{t}{\tau}\right)\right] \tag{3.7}$$

Where $\tau = \frac{\eta}{E_2}$, is the relaxation time, which is defined, as the time taken for the stress to fall to a value $\frac{1}{e} = \frac{1}{2.7}$ of the original stress. In other words it is a measure of how quickly a material recovers. From equation (3.7), it is clear that the strain is made up of two components. An instantaneous deformation corresponding to the spring, and a delayed response corresponding to the Kelvin element. This is illustrated in Figure 3.4.

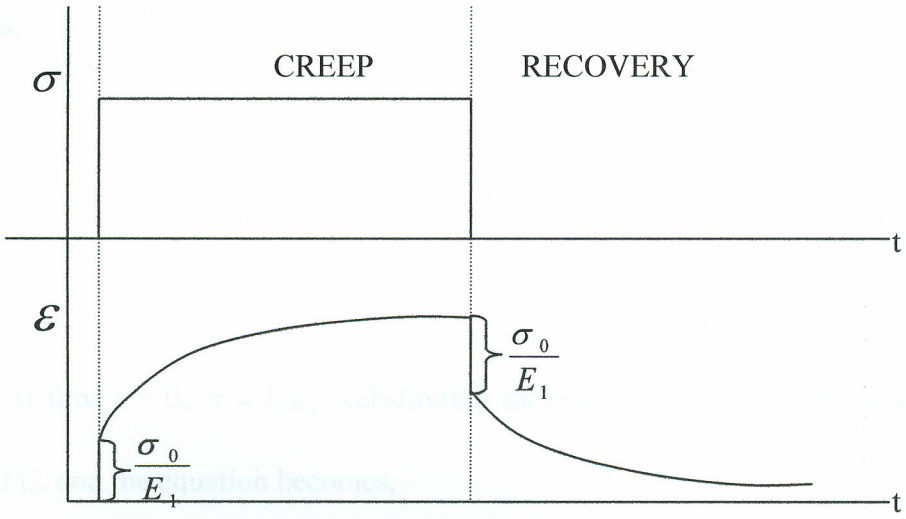

Figure 3.4; Creep response of a linear standard solid model

3.2.2 *Standard Linear Model Solution for Stress Relaxation*

This involves application of an instantaneous strain (ε_0), which is held steady while stress of the material is observed as a function of time. To obtain an expression for the corresponding stress we solve equation (3.3) holding strain constant, in this case the equation becomes,

$$E_1 E_2 \varepsilon_0 = \eta \frac{d\sigma}{dt} + (E_1 + E_2)\sigma \tag{3.8}$$

which can be rewritten as,

$$\frac{d\sigma}{dt} + \frac{\sigma}{\eta}(E_1 + E_2) = \frac{E_1 E_2 \varepsilon_0}{\eta} \tag{3.9}$$

Noting the equation has an integrating factor $e^{\frac{(E_1+E_2)t}{\eta}}$, we obtain an expression for the stress as,

$$\sigma e^{\frac{(E_1+E_2)t}{\eta}} = \frac{E_1 E_2 \varepsilon_0}{E_1 + E_2} e^{\frac{(E_1+E_2)t}{\eta}} + C \tag{3.10}$$

At time t = 0, $\sigma = E_1 \varepsilon_0$, substituting these values in (3.10) we can calculate the value of C, and the equation becomes,

$$\sigma(t) = \frac{E_1 \varepsilon_0}{E_1 + E_2}\left(E_2 + E_1 e^{\frac{-t}{\tau}}\right) \tag{3.11}$$

where $\tau = \frac{\eta}{E_1 + E_2}$, is the relaxation time. It can also be observed that the relaxation time depends on both spring stiffness and dashpot viscosity. Stress relaxes exponentially from a high initial value to a lower equilibrium value, as shown in the Figure 3.5.

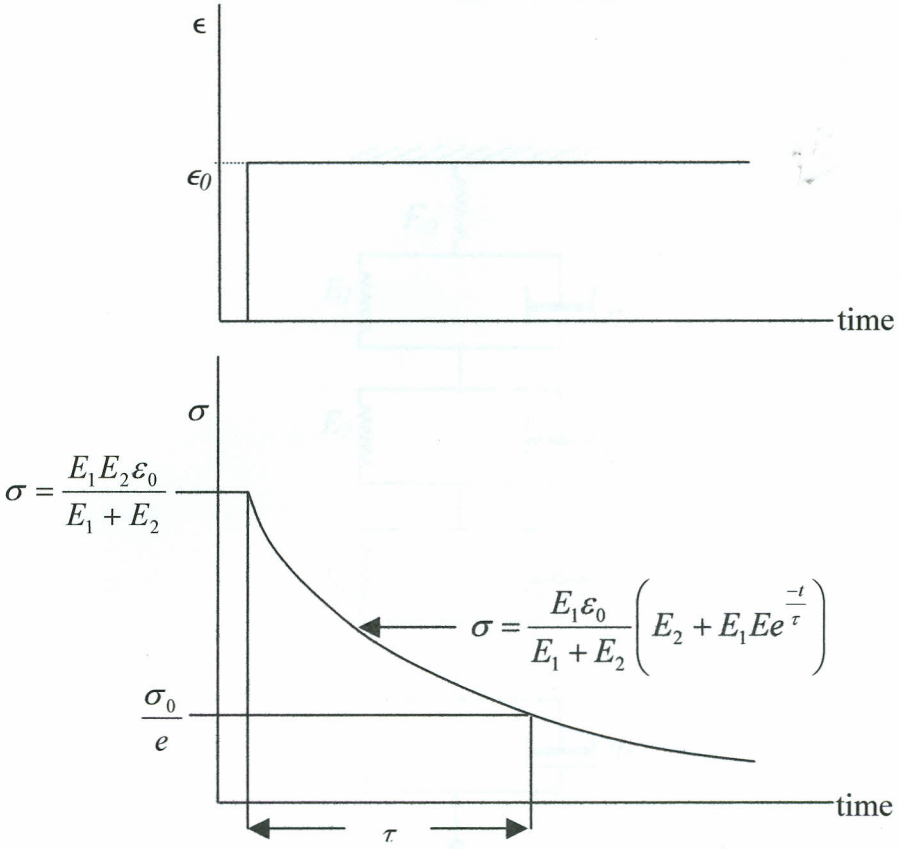

Figure 3.5; Stress relaxation response of an SLS model

The standard linear solid (SLS) model gives a good qualitative fit to creep and relaxation behavior of polymers, however the model incorporates only a single relaxation time, while in real polymers different lengths of chains respond differently, short chains respond faster than long ones. To model real polymers then, we may imagine a whole system of standard linear solids, each with its own relaxation time, (τ).

This behavior can be modeled by combining a number of elements into a multiple model, Figure 3.6 shows a series combination of a spring and several Kelvin elements.

Such a model has a finite number of components, giving a finite number of retardation times.

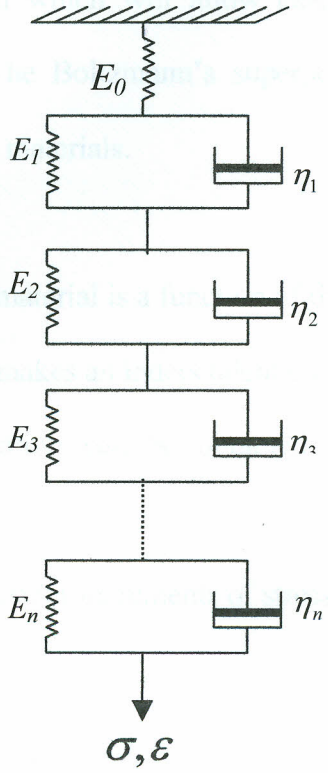

Figure 3.6; Multiple elements model for real materials

The expression of creep for the multiple model would be,

$$\varepsilon = \frac{\sigma_0}{E_0} + \sum_{i=1}^{n} \frac{\sigma_0}{E_i}\left(1 - e^{\frac{-t}{\tau_i}}\right) \tag{3.12}$$

where $\tau_i = \frac{\eta_i}{E_i}$ is the relaxation time for the ith Kelvin element.

3.2.3 *Boltzmann's Superposition Principle (Complex Loading Histories)*

Creep recovery and stress relaxation are responses to simple loading histories. A theoretical model is required which will allow calculation of the response to more complex loading histories. The Boltzmann's superposition principle is such a theory applying to linear viscoelastic materials.

Boltzmann proposed:

(i) The response of a material is a function of the entire loading history.

(ii) Each loading step makes an independent contribution to the final deformation.

(iii) The final deformation can be obtained by the simple addition of each contribution.

For creep experiments, we consider increments of stress with time.

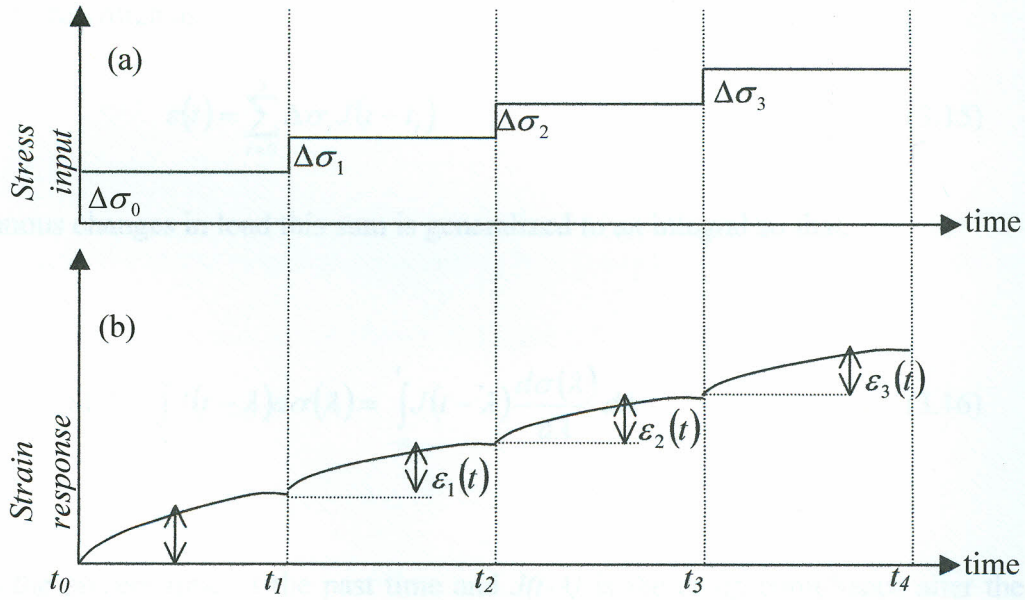

Figure 3.7 Boltzmann superposition principle;(a) applied stress history, (b) the resulting strain history, (McCrum et al, 1997; Ward and Hardley, 1993; Crawford, 1998)

Considering a staged loading program as the one in Figure 3.7,

$$\left.\begin{array}{l}\text{Response to } \Delta\sigma_0 \text{ at t=0 is } \varepsilon_0(t)=\Delta\sigma_0 J(t)\\ \Delta\sigma_1 \text{ at t=t}_1 \text{ is } \varepsilon_1(t)=\Delta\sigma_1 J(t-t_1)\\ \Delta\sigma_2 \text{ at t=t}_2 \text{ is } \varepsilon_2(t)=\Delta\sigma_2 J(t-t_2)\\ \Delta\sigma_3 \text{ at t=t}_3 \text{ is } \varepsilon_3(t)=\Delta\sigma_3 J(t-t_3)\end{array}\right\} \quad (3.13)$$

Where $J(t-t_i)$ is the creep compliance obtained from a simple single step loading creep test, hence the final deformation is given by the sum of these responses,

$$\varepsilon(t)=\Delta\sigma_0 J(t)+\Delta\sigma_1 J(t-t_1)+\Delta\sigma_2 J(t-t_2)+\Delta\sigma_3 J(t-t_3) \quad (3.14)$$

which can be rewritten as,

$$\varepsilon(t)=\sum_{i=0}^{3}\Delta\sigma_i J(t-t_i) \quad (3.15)$$

For continuous changes in load this sum is generalized to an integral so that,

$$\varepsilon(t)=\int_{-\infty}^{t} J(t-\lambda)d\sigma(\lambda)=\int_{-\infty}^{t} J(t-\lambda)\frac{d\sigma(\lambda)}{d\lambda}d\lambda \quad (3.16)$$

where t is the present time, λ the past time and $J(t-\lambda)$ is the creep compliance after the time interval $(t-\lambda)$. We integrate from $-\infty$ to t, in order to take into account all previous loading histories.

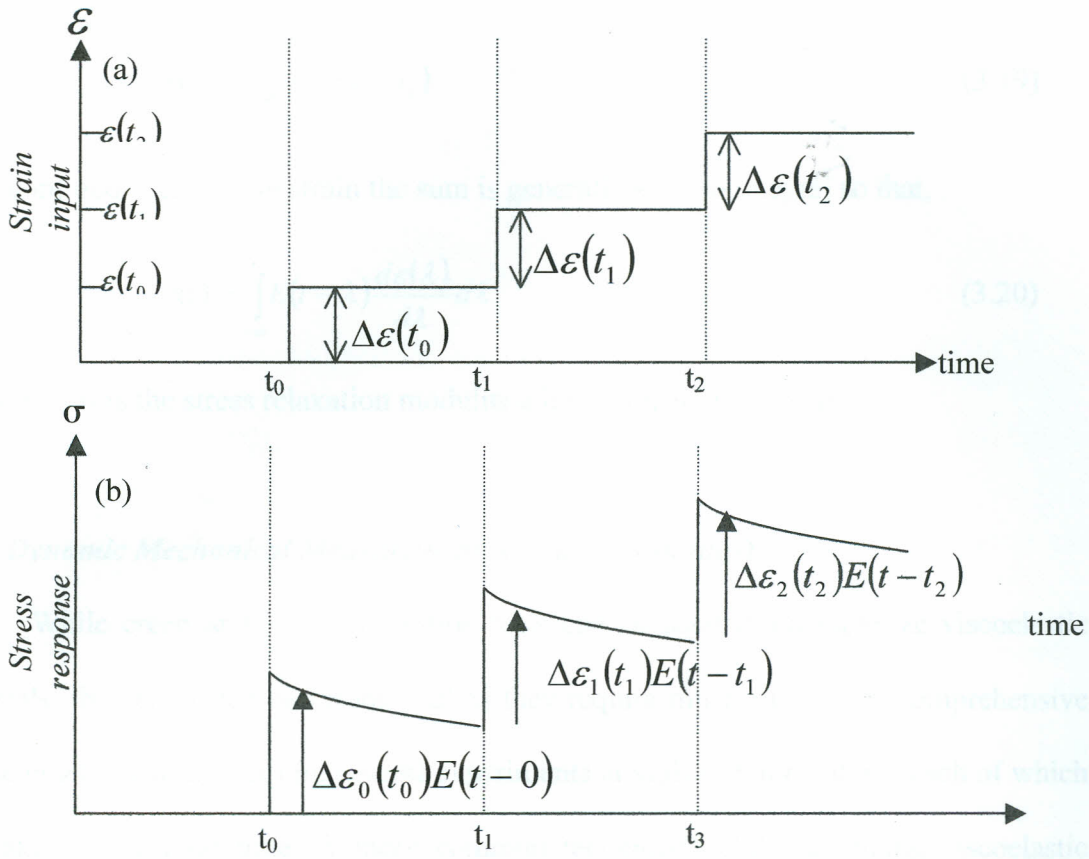

Figure 3.8 Boltzmann superposition principle; (a). Applied strain history (b) resulting stress history, (Fried, 1995; Sperling, 1992; Ward, 1993)

Similarly the stress response (relaxation) to a complex strain history involves an incremental addition of strain $\Delta\varepsilon$ as shown in Figure 3.8.

The response to $\Delta\varepsilon_0$ at t=0 is $\sigma_0(t) = \Delta\varepsilon_0 E(t-0)$

$\Delta\varepsilon_1$ at t=t_1 is $\sigma_1(t) = \Delta\varepsilon_1 E(t-t_1)$ (3.17)

$\Delta\varepsilon_2$ at t=t_2 is $\sigma_2(t) = \Delta\varepsilon_2 E(t-t_2)$

The final stress response is given by the sum of these responses,

$$\sigma(t) = \Delta\varepsilon_0 E(t) + \Delta\varepsilon_1 E(t-t_1) + \Delta\varepsilon_2 E(t-t_2) \tag{3.18}$$

which can be rewritten as,

$$\sigma(t) = \sum_{i=0}^{2} \Delta\varepsilon_i E(t - t_i) \tag{3.19}$$

For a continuous change in strain the sum is generalized to an integral so that,

$$\sigma(t) = \int_{-\infty}^{t} E(t-\lambda)\frac{d\varepsilon(\lambda)}{d\lambda} d\lambda \tag{3.20}$$

where $E(t-\lambda)$ is the stress relaxation modulus after a time interval $(t-\lambda)$.

3.2.4 *Dynamic Mechanical Measurement (Complex Modulus)*

While creep and stress relaxation tests can be used to characterize viscoelastic materials, they can often be impractical as they require much time since comprehensive characterization would require several experiments at various temperatures each of which can take a very long time. A more common technique of characterizing viscoelastic polymers is dynamic measurements. In this case measurements are done in the frequency domain, a sinusoidal stress is applied to the sample and the resulting strain is detected. Under such a regime two types of processes occur, namely storage and dissipation of energy. As a result, once equilibrium is attained, the strain will be out of phase with the stress response.

Suppose an oscillatory strain of angular frequency ω is generated in a polymeric sample then strain and stress both vary sinusoidally, however the strain lags behind the stress so that,

$$\text{strain} = \epsilon(t) = \epsilon_0 \sin \omega t \tag{3.21}$$

$$stress = \sigma(t) = \sigma_0 \sin(\omega t + \delta) \tag{3.22}$$

where δ is the phase angle. Equation (3.22) can be expanded to give

$$\sigma(t) = \sigma_0 (\sin \omega t \cos \delta + \cos \omega t \sin \delta) \tag{3.23}$$

From this expression it is clear that the stress consists of two components, one in phase with the strain and the other out of phase. We can rewrite equation (3.23) as,

$$\sigma(t) = \varepsilon_0 \left(\frac{\sigma_0}{\varepsilon_0} \cos \delta \sin \omega t + \frac{\sigma_0}{\varepsilon_0} \sin \delta \cos \omega t \right) \tag{3.24}$$

Equation 3.24 can be rewritten as

$$\sigma(t) = \varepsilon_0 (E' \sin \omega t + E'' \cos \omega t) \tag{3.25}$$

where $E' = \frac{\sigma_0}{\varepsilon_0} \cos \delta$ is the storage modulus defined as the energy stored due to the applied strain, it is a measure of the recoverable strain energy in a deformed body. $E'' = \frac{\sigma_0}{\varepsilon_0} \sin \delta$ is the loss modulus and it determines energy dissipation, which is a measure of the applied mechanical energy that is converted to heat through molecular friction. The tangent of the phase angle is called the loss factor. It is expressed as,

$$\tan \delta = \frac{E''}{E'} \tag{3.26}$$

Equation 3.26 represents a ratio of energy lost to the maximum energy stored per cycle, and is a measure of the damping properties of the material. The loss factor, storage modulus and loss modulus vary with frequency of loading as shown in Figure 3.9

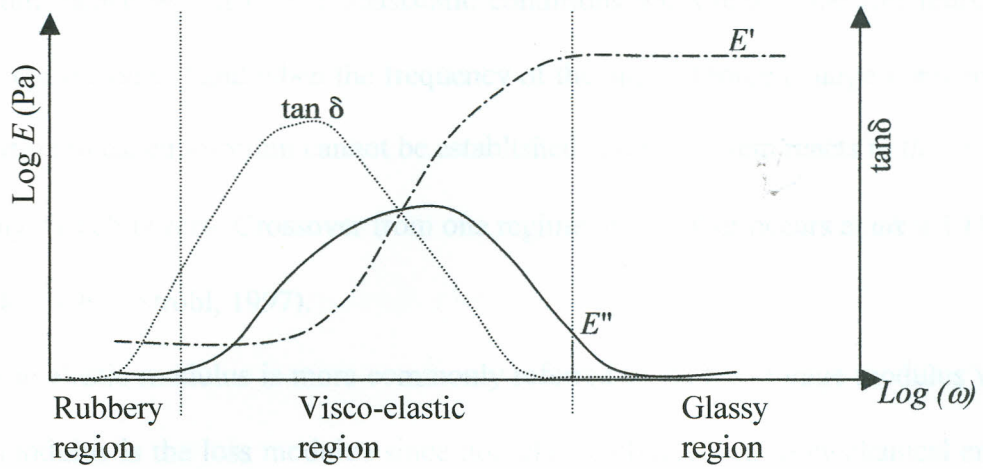

Figure 3.9 Storage modulus, Loss modulus and tan δ as a function of frequency, (Ward, 1993; McCrum, 1997)

At low frequency the polymer is rubber like and has a low storage modulus, which is independent of frequency. At high frequency, the polymer is glassy and the storage modulus is again independent of frequency. In the intermediate region where the material behaves viscoelasticaly, the storage modulus increases with increasing frequency. As the frequency is increased it becomes more difficult for the chains to respond to the applied forces and tend to remain in a frozen state. A frozen system stores more energy than a free to move system, (Ward and Hadley, 1993; Strobl, 1997; McCrum *et al*, 1997).

The loss modulus is zero both at low and at high frequencies where stress and strain are in phase for the rubbery and glassy phases. In the intermediate viscoelastic region, the loss modulus increases to a maximum value then decreases. If the mechanical force applied has a low frequency compared to the transition rates in the system, establishment of a thermal equilibrium is rapid and the system can always remain in

equilibrium, hence we encounter quasistatic conditions and observe the full relaxation strength. On the other hand when the frequency of the applied force is large compared to the transition rates, equilibrium cannot be established and the system reacts to the average strain only, which is zero. Crossover from one regime to the other occurs at $\omega\tau \cong 1$ (Ward and Hadley, 1993; Strobl, 1997).

The elastic modulus is more commonly referred to, as the storage modulus while viscous modulus is the loss modulus since non-elastic effects lead to mechanical energy losses. To be able to define the resultant dynamic modulus, it is appropriate to view stress and strain in a complex variable notation such that, (Sperling, 1992; Fried, 1995),

$$\varepsilon = \varepsilon_0 e^{i\omega t} \tag{3.27}$$

$$\sigma = \sigma_0 e^{i(\omega t+\delta)} \tag{3.28}$$

The complex modulus, E* is then given by,

$$E^* = \frac{\sigma}{\varepsilon} = \frac{\sigma_0 e^{i(\omega t+\delta)}}{\varepsilon_0 e^{i\omega t}} = \frac{\sigma_0 e^{i\delta}}{\varepsilon_0} = \frac{\sigma_0}{\varepsilon_0}(\cos\delta + i\sin\delta) = \frac{\sigma_0}{\varepsilon_0}\cos\delta + i\frac{\sigma_0}{\varepsilon_0}\sin\delta = E' + iE'' \tag{3.29}$$

3.2.5 *Temperature Dependence of the Relaxation Time*

Temperature dependence of polymer properties is of great importance because the physical and mechanical properties of polymers change drastically as temperature changes. It is important to study relaxation behavior of polymers, at a particular temperature for a given time period. Unfortunately, the time window in which complete viscoelastic behavior of the material can be accessible is impractical. The temperature

dependence of the relaxation time provides a way of varying the temperature window so as to bring the relaxation process within a time scale that is readily accessible. Viscoelastic behavior at short or long time periods can be predicted by extrapolation. Changes due to temperature can be described in terms of free volume or relaxation time. At temperatures below T_g, local chain relaxation takes place. At these temperatures motions are hindered by close presence of other molecules. For relaxation to take place a potential barrier must be surmounted. In this region the kinetics of relaxation are better described on the basis of barrier state theories as such the temperature dependence of the relaxation time τ is often described by the Arrhenius equation as (Sperling, 1992; Fried, 1995; McCrum *et al*, 1997)

$$\tau = \tau_0 \exp\left[\frac{\Delta U}{kT}\right] \tag{3.30}$$

τ_0 is the pre-exponential factor, ΔU the activation energy, k is the Boltzmann constant and T is the absolute temperature.

In contrast to local motions, relaxation times associated with secondary motions are dependent on free volume. The presence of free volume allows the molecules to relax to a new configuration. The Doolittle equation gives a relation that expresses the dependence of relaxation time on the free volume as (Doolittle *et al,* 1957),

$$\tau = \tau_0 \exp\left(\frac{BV_0}{V - V_0}\right) \tag{3.31}$$

Where V is the total volume, V_0 is the occupied volume, $B = \xi\left(\frac{V^*}{V_m}\right)$ is a constant given

by Cohen Turnbull free volume theory, V^* is the minimum volume required for relaxation process to take place, V_m is the mean volume of relaxing polymer segment. ξ is a constant such that, $0.5<\xi<1$ (Cohen and Turnbul, 1954).

Since the total volume V is a linear function of temperature, then V can be expressed as,

$$V = V_0 + \alpha(T - T_0) \tag{3.32}$$

where α is the volume thermal expansion co-efficient. Substituting equation (3.32) into (3.31) we obtain,

$$\tau = \tau_0 \exp\left(\frac{BV_0}{\alpha(T - T_0)}\right) = \tau_0 \exp\left(\frac{K}{T - T_0}\right) \tag{3.33}$$

where $K = \left(\frac{BV_0}{\alpha}\right)$ is a constant, T_0 is the absolute temperature at which free volume would be zero and τ_0 is the characteristic time at which free volume would be zero.

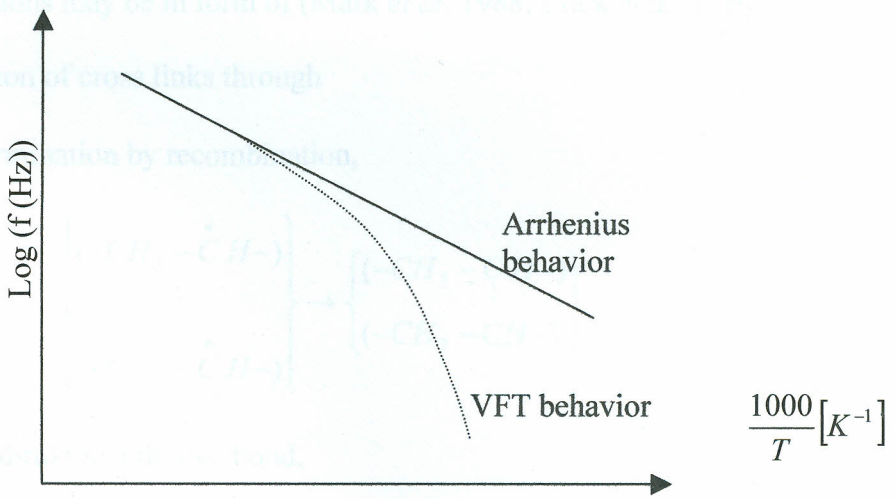

Figure 3.10 Comparison of the Arrhenius and VFT relationship (Sperling, 1992; McCrum et al, 1997)

Equation (3.33) is known as the Vogel Fulcher Tamann (VFT) equation. A comparison of the Arrhenius and VFT relationship is shown in Figure 3.10. At high temperatures the two are approximately the same but differ significantly at lower temperatures.

3.3 Irradiation of the Samples

Modification in polymeric molecular structure can be brought about by either conventional chemical means, usually involving silanes or peroxides, or by exposure to ionizing radiation from either radioactive sources or highly accelerated electrons. Ionizing radiation interacts with matter by transferring energy to the electrons orbiting the atomic nucleus of the target material. These electrons may then be released from the atoms yielding positively charged ions and free electrons, or moved to a higher-energy atomic orbital, yielding an excited atom or molecule (free radical). These radicals then participate in reactions that are important in altering the polymer structure and properties, these reactions may be in form of (Mark *et al*, 1988; Mark *et al*, 1986),

(i) Formation of cross links through

- Termination by recombination,

$$\left\{\begin{array}{l}(-CH_2-\dot{C}H-)\\ +\\ (-CH_2-\dot{C}H-)\end{array}\right\}\rightarrow\left\{\begin{array}{l}(-CH_2-\underset{|}{C}H-)\\ (-CH_2-CH-)\end{array}\right\}$$

- Addition to a double bond,

$$\left\{\begin{array}{l}(-CH_2-\dot{C}H-)\\ +\\ (-CH=CH-)\end{array}\right\}\rightarrow\left\{\begin{array}{l}(-CH_2-\underset{|}{C}H-)\\ (-\dot{C}H\ -CH-)\end{array}\right\}$$

(ii) Fracture of the main chain, there by causing chain scission,

$$\left(-CHR-CH_2-\dot{C}R-CH_2-\right)\rightarrow\left(-CHR\bullet+CH_2=CR-CH_2-\right)$$

During irradiation, chain scissioning occurs simultaneously and competitively with cross linking, the end result being determined by the ratio of the yields of the two reactions. However, generally polymers containing a hydrogen atom at each carbon atom predominantly undergo crosslinking while those with quaternary carbon atoms and polymers of the form $(-CH_2-CR_2-)$, where R is a side group different from hydrogen, undergo chain scission (Messick, 2003; Burton *et al*, 1960). Aromatics, like polystyrene and polycarbonate are relatively resistant (Mark *et al*, 1986). However polyolefins such as polyethylene, polypropylene and polyvinylchloride, are known to crosslink as well as degrade (Burton *et al*, 1960).

It is important to note that gamma ray irradiation doses do not require catalysts, so there are no catalyst residues in the final product to interfere with physical properties of the material. It also does not involve heat treatment that could degrade thermally sensitive components.

3.4 Radiation Dosimetry

3.4.1. *Exposure*

Exposure is defined for gamma rays in terms of the amount of ionization they produce in air, which is taken as the total electrical charge (the ionization) produced in a given mass (or volume) of air. The unit of exposure is the roentgen (*R*), defined as,

$$1\text{R} = 2.58 \times 10^{-4}\text{C/kg} \qquad (3.34)$$

where, the charge and mass in the definition of roentgen refer only to air. We can find the energy absorbed per unit mass of air per roentgen of exposure. Since the electronic charge is $1.60 \times 10^{-19} C$, equation (3.34) gives for the number of ion pairs (ip) produced per kg of air for an exposure of $1R$ as

$$1R = \frac{2.58 \times 10^{-4} C}{kg} \times \frac{1}{1.60 \times 10^{-19} C / ip} = 1.61 \times 10^{15} \frac{ip}{kg} \qquad (3.35)$$

The concept of exposure and the definition of the roentgen provide a practical, measurable standard for electromagnetic radiation in air. However additional concepts are needed for it to apply to tissue. Tissue in this case refers to material other than air (James, 1986)

3.4.2 *Absorbed Dose*

The absorbed dose is the energy absorbed per unit mass from any kind of ionizing radiation in matter, usually referred to simply as dose. Its SI unit is the Gray (Gy).

$$1\text{Gy} \equiv 1\text{J/Kg} = (10^7 \text{ erg}/10^3 \text{ g}) = 10^4 \text{ erg/g} = 100 \text{ rad} \qquad (3.36)$$

3.4.3 *Dose Rate*

To formulate an expression for computing the dose rate in tissue from a gamma source of strength C curies that emits an average photon energy of E MeV per disintegration, a brief theory is presented here from J.E.Turner (James, 1986). The rate of energy release in the form of photons escaping from the source is,

$$CE\ (CiMeV) \times \frac{3.7 \times 10^{10}}{\sec Ci} \times \frac{1.6 \times 10^{-6}\ erg}{MeV} = 5.92 \times 10^4 CE\ \frac{erg}{\sec} \qquad (3.37)$$

Neglecting attenuation in air, the rate of energy flow per unit area (=intensity) through the surface of a sphere of radius *r (cm)* surrounding the source is,

$$I = \frac{5.92\times10^{4}CE}{4\pi r^{2}} = \frac{4.71\times10^{3}CE}{r^{2}}\frac{erg}{cm^{2}\,\sec} \tag{3.38}$$

The rate of energy absorption in a volume element of air having unit area and thickness *dr* at *r* (Fig 3.11) is given by $I\mu_A dr$, where μ_A is the average energy absorption coefficient in cm^{-1} for the photons, if the density of air is ρ g/cm^3, then the mass of air in the volume element is, ρ dr grams.

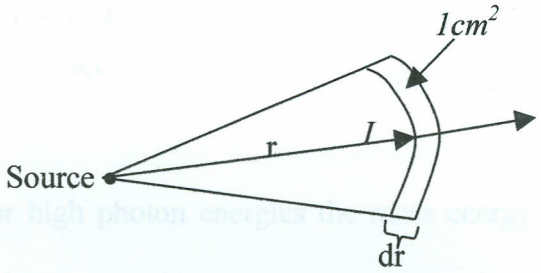

Fig 3.11: *Rate of energy absorption by air thickness dr per cm^2 is $I\mu_A dr$, where μ_A is the energy absorption coefficient cm^{-1}, (James, 1986)*

and absorbed dose rate

$$\dot{D} = \frac{I\mu_A dr}{\rho\, dr} = \frac{4.71\times10^{3}CE\mu_A dr}{r^{2}\rho\, dr}\frac{erg/cm}{cm^{2}\,\sec g/cm^{3}} = \frac{4.71\times10^{-3}CE\mu_A}{r^{2}\rho}\frac{erg}{g\,\sec} \tag{3.39}$$

At STP, ρ = 0.001293g/cm^3, and so converting to rad, we have,

$$\dot{D} = \frac{4.71\times10^{3} CE\mu_A}{r^2 \times 0.001293}\frac{erg}{g\,\sec} = \frac{3.64\times10^{4} CE\mu_A}{r^2}\frac{rad}{\sec} \qquad (3.40)$$

This is an appropriate expression for gamma dose rate over the Compton range of photon energies for which the energy absorption coefficient μ_A is approximately constant. For photon energies ~ 60 keV – 2 MeV, the mass absorption coefficient of air is approximately, $\left[\frac{\mu_A}{\rho}\right] \cong 0.027\text{cm}^2/\text{g} \Rightarrow \mu_A \cong 3.5\times10^{-5}\text{cm}^{-1}$.

$\dot{D} \cong 1.27CE$ rad, On substituting this in equation (3.40) one obtains,

$$\dot{D} \cong \frac{1.27CE}{r^2}\frac{rad}{\sec} \qquad (3.41)$$

Since for high photon energies the mass energy absorption coefficient of water $\left(\frac{\mu_W}{\rho}\right)_W$ is equal to the mass energy absorption coefficient of polyethylene $\left(\frac{\mu_P}{\rho}\right)_P$ (ICRU Report, 1970). The dose absorbed by polyethylene was calculated using the expression,

$$\dot{D}p = \dot{D}w\left(\frac{(\mu_P/\rho)_P}{(\mu_W/\rho)_W}\right) \qquad (3.42)$$

which means that

$$\dot{D}_P = \dot{D}_W \tag{3.43}$$

where $\dot{D}_W$ is the absorbed dose in water and $\dot{D}_P$ is the absorbed dose in medium.

3.5 DMA Measurement System

The DMA measurement system consists of four components

- A linear force motor: This provides precise control of all stresses applied to the sample. The high resolution of the motor allows for reproducible force control. It supplies the sinusoidal deformation force to the material.
- Furnace: This controls the temperature of the system.
- The central core rod (drive shaft): This is the device through which all stresses are applied to the sample from the drive motor. It transfers the force from the drive motor to the clamps that hold the sample.
- Mechanically controlled displacement detector: This is the one that accurately tracts any mechanical changes occurring in the sample due to changes in temperature atmosphere and time. It then detects changes in the system's resonance frequency and supplies electrical energy needed to maintain the preset amplitude. The amount of electrical energy supplied is a measure of the damping properties of the material. Changes detected are then expressed in terms of current, which are then easily separated by a phase sensitive detector and hence the signals can be measured.

3.6 DSC Measurement Technique

The DSC measures the temperature and heat flow associated with transitions (for example glass transition or melting temperatures) in materials as a function of heat flow and temperature. It is based on the fact that whenever a material (for example a polymer) undergoes a physical or chemical change a corresponding change in enthalpy is observed. (Sperling, 1992; Fried, 1995). The experimental sample and reference sample containers are mounted on their respective heaters and temperature sensors. The two containers are air tight and thermally isolated from each other and also from the environment.

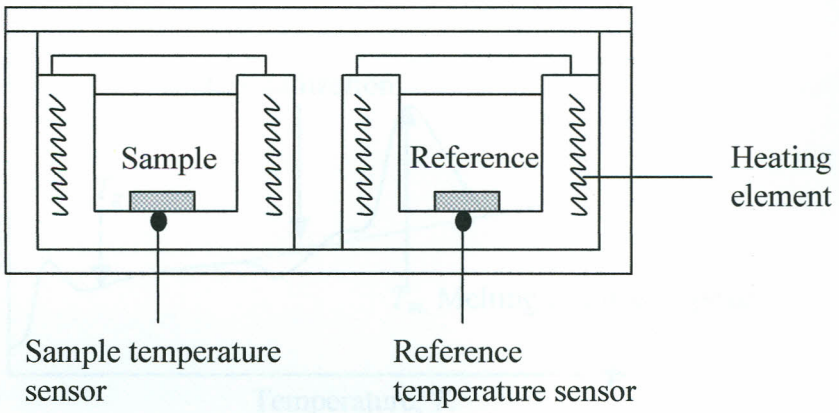

Figure 3.12 Schematic representation of differential scanning calorimetry measuring cells

The measurement condition for the DSC is that at any given time, the temperature of the sample (T_S) and that of the reference sample (T_R) always remains the same so that

$$T = T_S = T_R \tag{3.44}$$

For this to be maintained the heating rate of the system keeps changing. Supposing the heating rate is adjusted to some value ψ the temperature of the whole system at any given time t is

$$T = T_0 + \psi t \tag{3.45}$$

where T_0 is the temperature at time $t=0$

The difference in electrical power ΔQ supplied in order to maintain the reference and sample pans at equal temperature during programmed heating cycle, is then recorded as a function of temperature (T), and time (t). The displayed thermogram in Figure 3.14 is a profile of the instantaneous rate of change of ΔQ, $d(\Delta Q)$, against temperature.

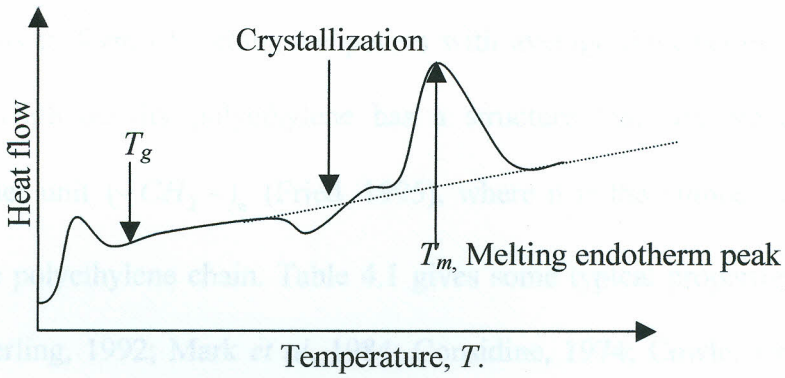

Figure 3.13 An illustration of a DSC thermogram, (Stevens, 1990; Sperling, 1992; Fried, 1995)

In this method, T_g appears as a shift in the baseline, and melting and crystallization, as exothermic and endothermic peaks respectively.

CHAPTER 4

EXPERIMENTAL TECHNIQUES

4.1 Introduction

This chapter describes the materials, sample preparation, apparatus used for sample irradiation, and experimental procedures adopted for the DMA measurements.

4.2 Materials

Virgin high density polyethylene (VHDPE) and recycled high density polyethylene (RHDPE) used was provided by Drum and Container Plastic Company in Ruiru, Kenya. VHDPE was in form of spherical milky pellets of average diameter 2mm, while RHDPE was in form of rectangular pellets with average dimensions of 4mm by 2mm by 1mm. High density polyethylene has a structure that consists of a linear repeating monomer unit $(-CH_2-)_n$ (Fried, 1995), where n is the number of repeating units forming the polyethylene chain. Table 4.1 gives some typical properties of HDPE (Fried, 1995; Sperling, 1992; Mark *et al*, 1984; Considine, 1974; Cowle, 1991; Danch, 2003).

Table 4.1; Typical physical properties of HDPE

PROPERTY	RANGE
Melting temperature, T_m *(K)*	400 - 408
Specific gravity, g/cm^3	0.95 – 0.97
Molecular weight, *g/mole*	200,000 – 500,000
Glass transition, T_g *(K)*	140 -180

4.3 Sample Preparation

4.3.1 Mold

The mold used to prepare the samples had been locally made in the Kenyatta University Science Workshop. It consisted of two thick aluminum plates each measuring 150 mm by 150 mm with a non-stick coating on the inner surfaces of the mold. The mold also had four holes on all the corners where fastening screws were fitted. In addition the mold had four identical rings of 2.5 mm in thickness and a diameter of 10 mm. The rings acted as spacers for the aluminum plates, and they were held in position by the fastening screws. This made it possible to obtain polymer molds of even thickness. The mold also had a 5 mm hole at the center of one of the plates, where the injection of the polymer melt was done. Figure 4.1 shows the top and side views of the mold used.

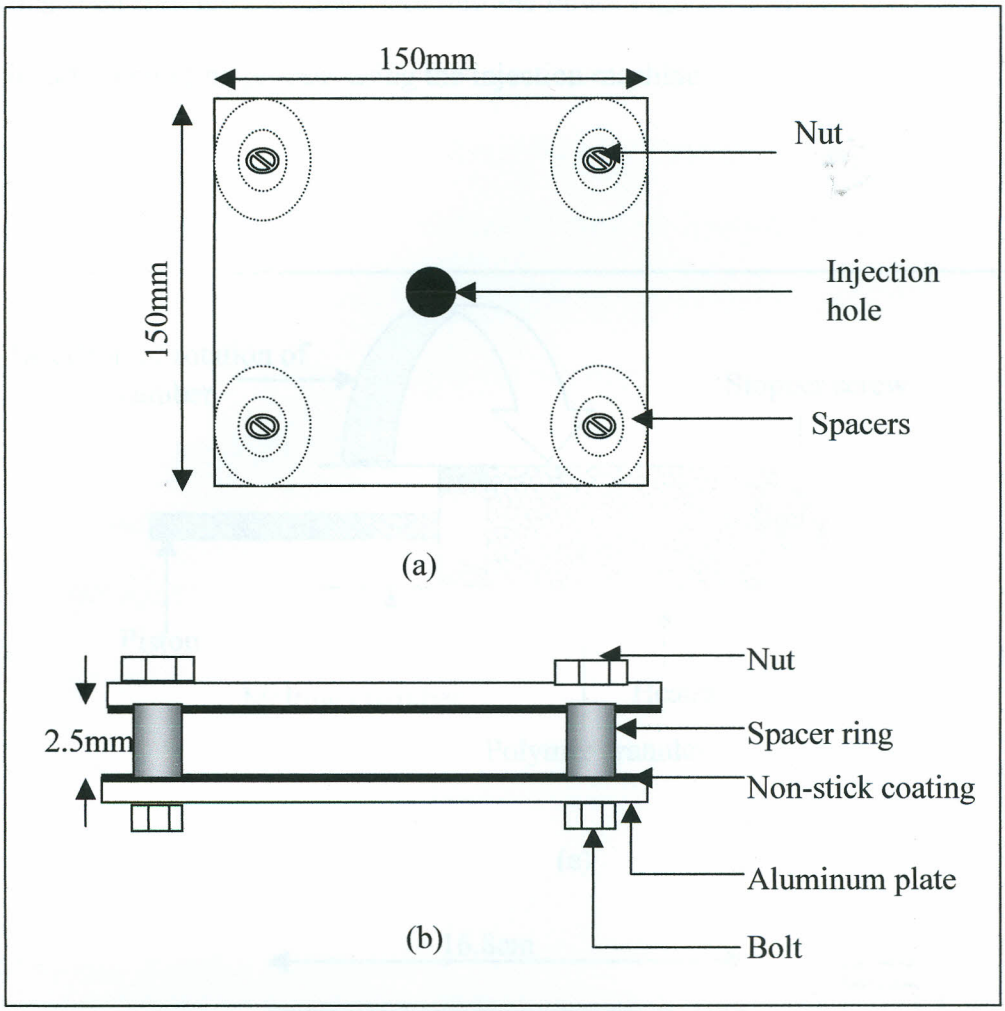

Figure 4.1 Mold; (a) top view (b) side view

4.3.2 *Injection Machine*

The injection machine consisted of a cylindrical melting chamber made from brass. It had a length of 168 mm and diameter of 18 mm. It was open on one side but the other side was closed leaving a 5mm diameter hole from where injection of the polymer melt was done. A stopper screw to fit into the hole was used during the heating process and removed just before the polymer melt was injected into the mold. The machine also had a piston that fitted on the open end of the melting chamber. This was used to push the

polymer melt through the small hole into the mold. Figure 4.2 shows the heating process and injection molding process using the injection machine.

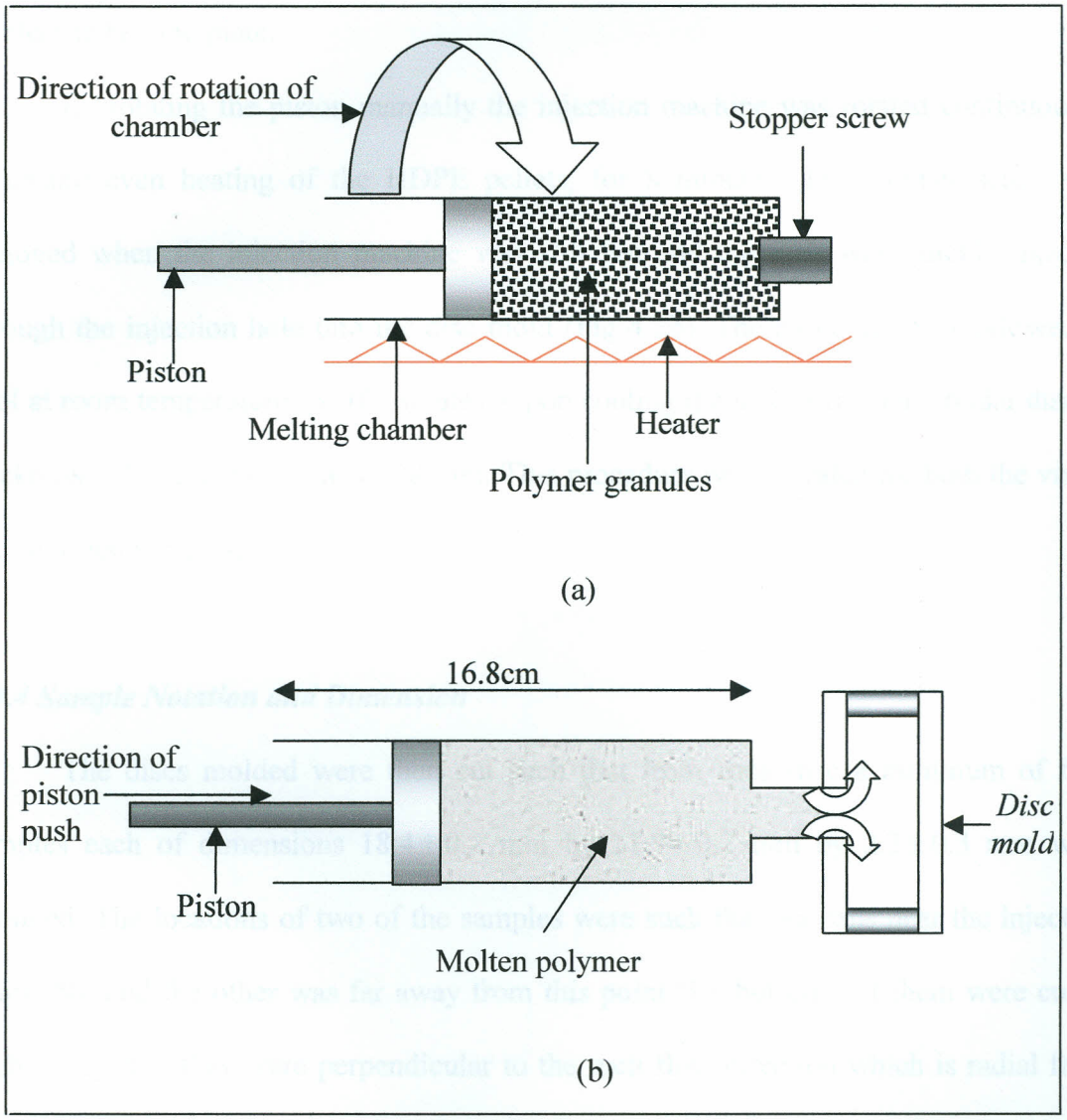

Figure 4.2 Injection molding machine; (a) Heating process (b) Injection molding process

4.3.3 Sample Molding

The stopper screw was fitted on the injection machine and then 15 g of HDPE pellets were put into the melting chamber, (Fig 4.2a). The piston was then inserted in the melting chamber through the open end, and finally the injection machine was placed on an electric heating plate.

By rotating the piston manually the injection machine was rotated continuously, to ensure even heating of the HDPE pellets, for 8 minutes. The stopper screw was removed when the injection machine was still hot and the melt was quickly injected through the injection hole into the disc mold (Fig 4.2b). The mold was then allowed to cool at room temperature for 10 minutes. Upon cooling the melt formed a circular disc of thickness 2.25 mm and diameter 78 mm. This procedure was repeated for both the virgin and recycled samples.

4.3.4 Sample Notation and Dimension

The discs molded were then cut such that from each disc a minimum of four samples each of dimensions 18.4 ± 0.2 mm by 11.9 ± 0.2 mm by 2.2 ± 0.3 mm were obtained. The locations of two of the samples were such that one was near the injection point (N), and the other was far away from this point (F), but both of them were cut in such a way that they were perpendicular to the melt flow direction which is radial from the injection point. The other two samples were cut such that one was along the flow direction (A), and the other perpendicular to the flow (P). The samples were identified using a combination of the alphabetical and numerical notation. The first letter was either a V or an R, which indicated whether the sample in question was from virgin HDPE or

from recycled HDPE. Next to the letter was a number 0, 1 or a 2, this represented the dose of the sample in question. By multiplying the indicated number by 6, one obtains the actual dose of the sample in krad. The third letter was representative of the position from which the sample was cut, an A represents a sample that is cut along, N a sample cut near the injection point, F a sample cut far away from the injection point and P a sample cut perpendicular to the injection point. Using this notation to represent a sample cut near the injection point from a recycled HDPE disc, that is irradiated to a dose of 6 krad, notation R1N was used.

The nomenclature, directions and dimensions to characterize each sample are shown in Figure 4.3.

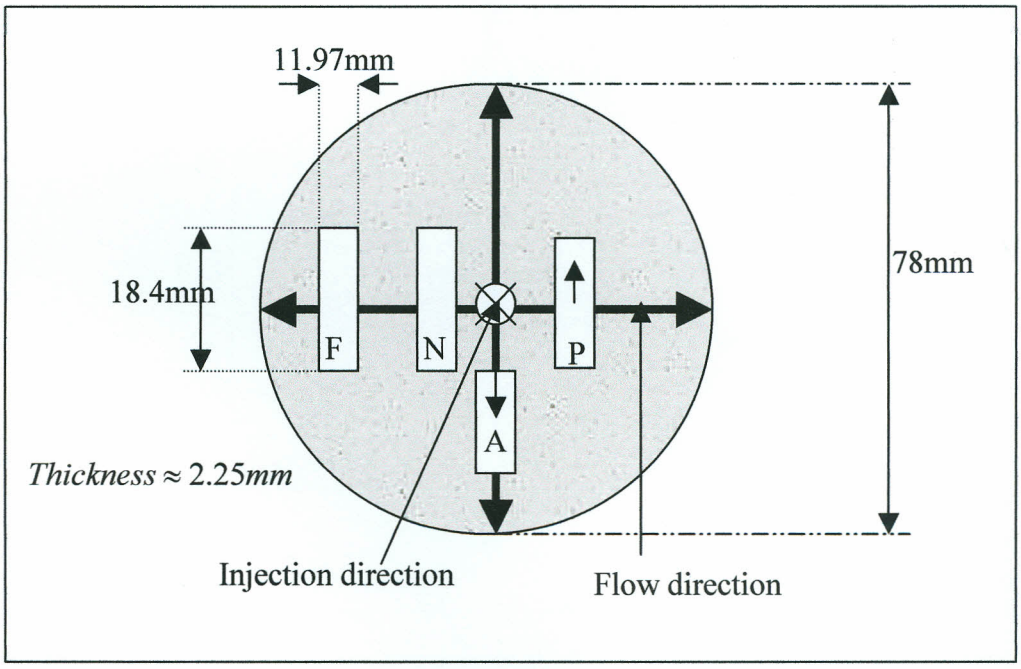

Figure 4.3 *Samples nomenclature and dimensions*

4.3.5 Sample Irradiation

The Gamma ray irradiation of the samples was carried out at Nairobi Hospital using a Cobalt 60 teletherapy unit, model Shimadzu RTGS – 21, source with a field size of 120 mm by 120 mm at a distance of 650 mm from the source. The dose rate of the source was 1.528 Gy/min. Water was used to cover the samples up to a depth of 5 mm. The water simulates the calibration condition, and also helps in scattering the radiation. The samples were put 5mm under water since the dose is maximum at a depth of 5mm from the surface. The Cobalt 60 teletherapy unit equipment had an uncertainty of $\pm 3\,\%$, which was last verified on 13-7-2000 by the International Atomic Energy Agency (IAEA). Figure 4.3a below shows the equipment used and the set up for the irradiation process. Figure 4.3b shows the details of the various dimensions for the set up.

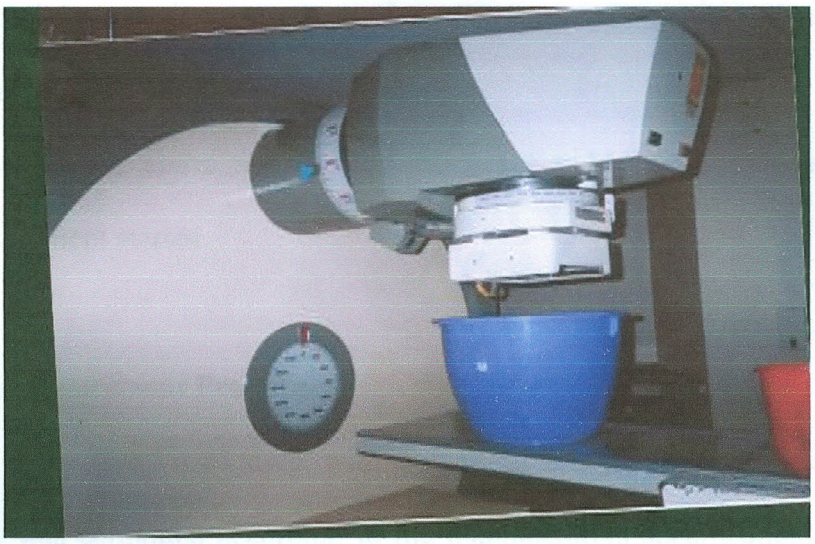

(a)

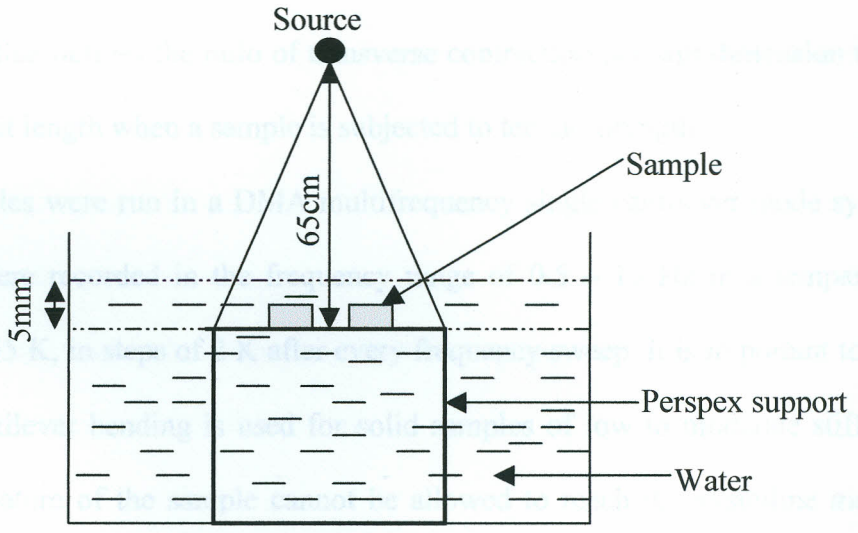

(b)

Figure 4.4 Gamma ray radiation apparatus set up; (a) A photograph to show the Cobalt 60 teletherapy equipment and the set up for irradiation, (b) Set up for irradiation.

To attain a dose of 0 krad the samples were not exposed to any radiation, to attain one of 6 krad the samples were exposed for 2356 seconds and for a dose of 12 krad for 4712 seconds.

Once all the above sample preparation stages had been undertaken, DMA and DSC measurement started.

4.4 DMA Measurement Procedure

A DMA 2980 was used with a thermal analysis software version 4.0. The instrument was calibrated according to the manufacturers specifications, as outlined in the users manual. The instrument parameter was set at 0.44 and data sampling at interval of 2.0 sec/point. In this case instrument parameter refers to the Poisson's ratio, which is a DMA parameter that defines the ratio of transverse contraction per unit dimension to the elongation per unit length when a sample is subjected to tensile strength.

The samples were run in a DMA multifrequency single cantilever mode system. Measurements were recorded in the frequency range of 0.5 – 13 Hz in a temperature range of 298 – 355 K, in steps of 2 K after every frequency sweep. It is important to note here that the cantilever bending is used for solid samples of low to moderate stiffness, hence the temperature of the sample cannot be allowed to reach its crystalline melting temperature.

The sample was clamped as shown in Figure 4.5. After this, measurement started.

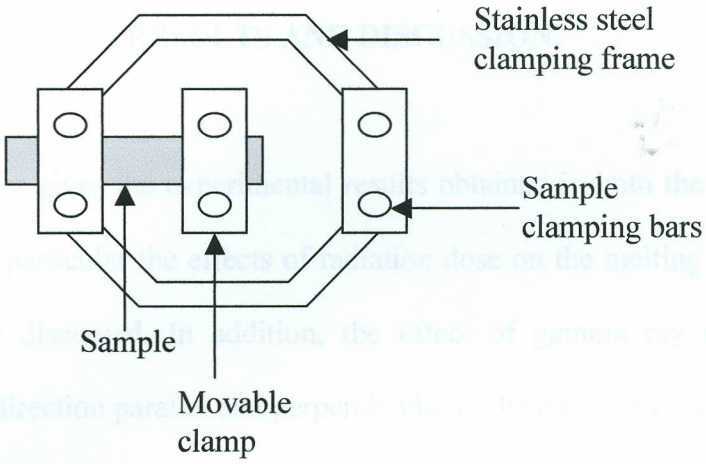

Fig 4.5 Front view (vertical horizontal) of a single cantilever

4.5 DSC Measurement Procedure

DSC measurement was done with the help of Ms Westphal of University of Leipzig (Germany).

The experimental sample was fitted into the sample container. The experimental sample container and the reference sample containers were then mounted on their respective heaters and temperature sensors. DSC thermograms were then obtained at a heating rate of 10 K/min from 270 K to 410 K.

CHAPTER 5

RESULTS AND DISCUSSION.

5.1 Introduction

This chapter gives the experimental results obtained in both the DMA and DSC measurements. In particular the effects of radiation dose on the melting temperature and loss modulus are discussed. In addition, the effect of gamma ray radiation on the anisotropy in the direction parallel and perpendicular to the melt flow and anisotropy near and far away from the injection point are also discussed. The data presented is from selected frequencies for the purpose of a clear comparison.

Taking the measurement of three unirradiated samples and comparing their curves as shown in Figure 5.1 one obtains the uncertainty in the DMA data. The uncertainty is found to be ± 4.13 MPa. The observed error could have resulted in that the point of clamping may not be exactly identical. At the same time the DMA is very sensitive to dimensions as such any slight difference in the sample dimension could affect the results obtained.

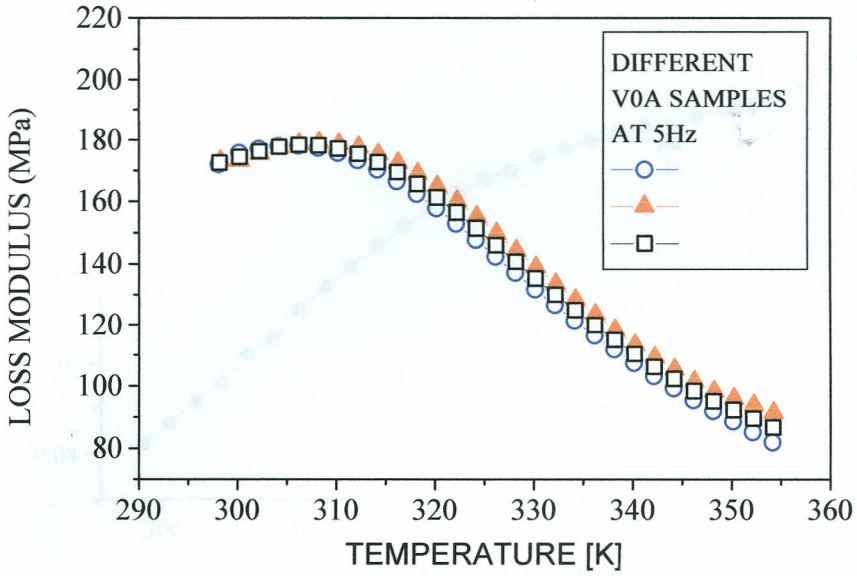

Figure 5.1: The loss modulus, as a function of temperature at a frequency of 0.5Hz for three different V0A samples

Using the data obtained for V0A, one can also plot the graph of Tan δ against temperature. The curve obtained at a frequency of 1Hz is as shown in Figure 5.3. The curve gives the peak position of the β relaxation as 337.93 K. This value is close to the value of 333 K obtained at the same frequency by Flocke, using a torsion pendulum (Flocke, 1962).

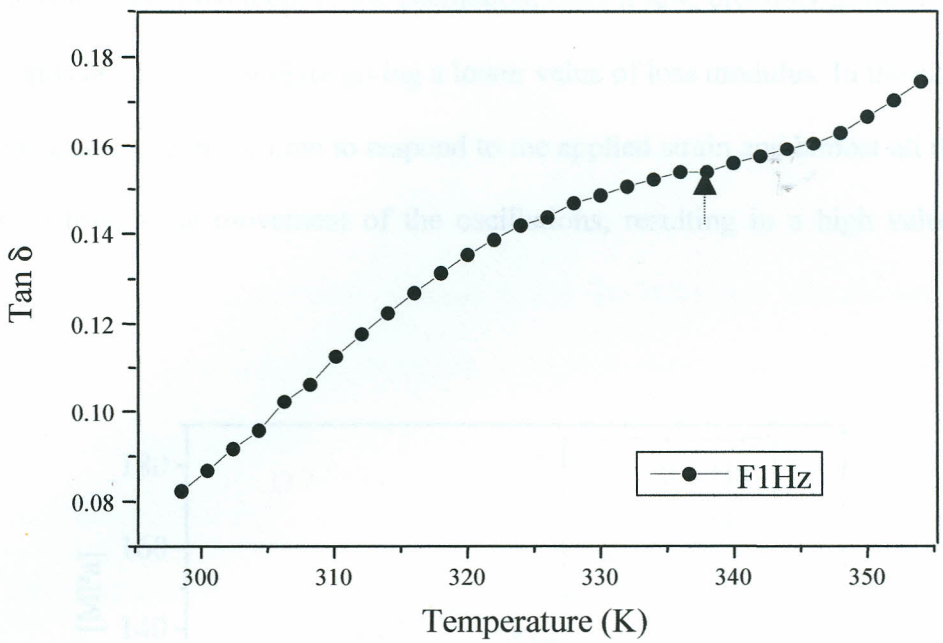

Figure 5.2: Temperature dependence of the loss tangent for V0A obtained at 1Hz

5.2 Effects of Frequency and Temperature on the Loss Modulus of Unirradiated Sample (V0A)

Figure 5.1 shows a plot of the loss modulus versus temperature for the β process at different frequencies. It is important to mention here that β relaxations in polyethylene originate from the amorphous part of the semi-crystalline polymer and it involves the onset of glass transition in these regions (Strobl, 1997; Billmeyer, 1984). It is observed that the peak of the loss modulus decreases in intensity as the frequency increase, but shift to higher temperatures.

This decrease in the intensity of the loss modulus peak as frequency is increased can be attributed to the fact that at high frequencies the chains are not allowed enough time to respond to the applied sinusoidal strain and it becomes quite difficult for the

chains to follow the movement of the oscillation. Only a few, probably those with shorter chain lengths are able to oscillate giving a lower value of loss modulus. In the case of low frequency, chains are given time to respond to the applied strain and almost all the chains are able to follow the movement of the oscillations, resulting in a high value of loss modulus.

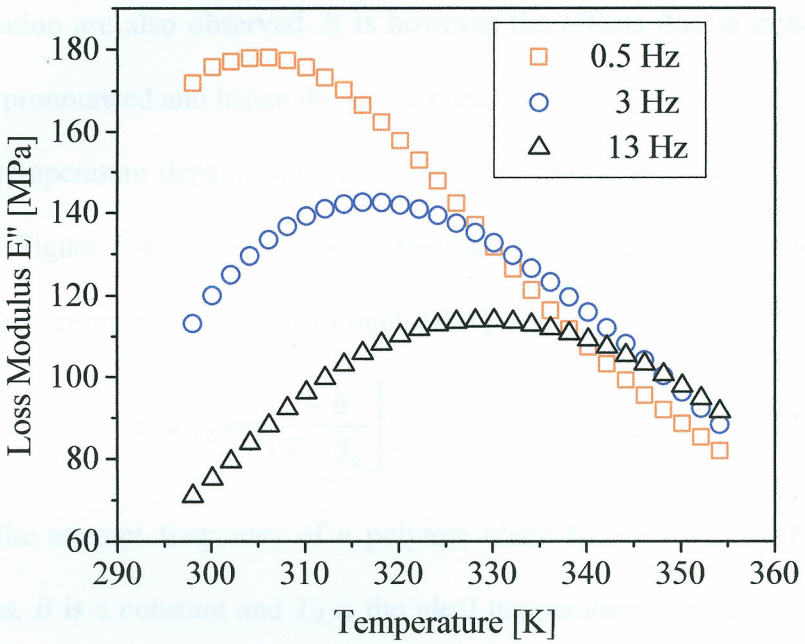

Figure 5.3: Loss modulus, as a function of temperature at different frequencies

As the temperature increases the polymer softens allowing more chains to take part in the oscillations and hence an increase in the loss modulus is initially observed, however, HDPE being a highly crystalline material crystallizes when the temperature is raised above the glass transition temperature, T_g. Temperature increase enables substantial parts of the chain to extricate themselves from their entanglements and align

themselves in a more cohesive crystalline manner, (Stevens, 1990; Billmeyer, 1984; Hay, 1995). This formation of crystallites affects the segmental mobility due to restrictions and limitations imposed by crystallites and trapped entanglements, as a result the number of chains participating in the relaxation process reduces thus reducing the loss modulus. It is therefore evident that, temperature increase makes the relaxation process faster due to softening of the polymer however, decreases in intensity due to chain constraints imposed by crystallization are also observed. It is however the effects due to crystallization that are far more pronounced and hence the above observation.

The temperature dependence of the mean relaxation frequency for the process is as shown in Figure 5.4. It can be noted that the temperature dependence follows the Vogel Fulcher-Tammann (VFT) law (Vogel, 1921)

$$f = f_0 \exp\left[\frac{-B}{T - T_0}\right] \tag{5.1}$$

where f_0 is the attempt frequency of a polymer chain before it finally responds to the applied stress, B is a constant and T_0 is the ideal temperature, which is 50 ^0C below the calorimetric T_g (Danch, 2003). The fit parameters are included in the graph.

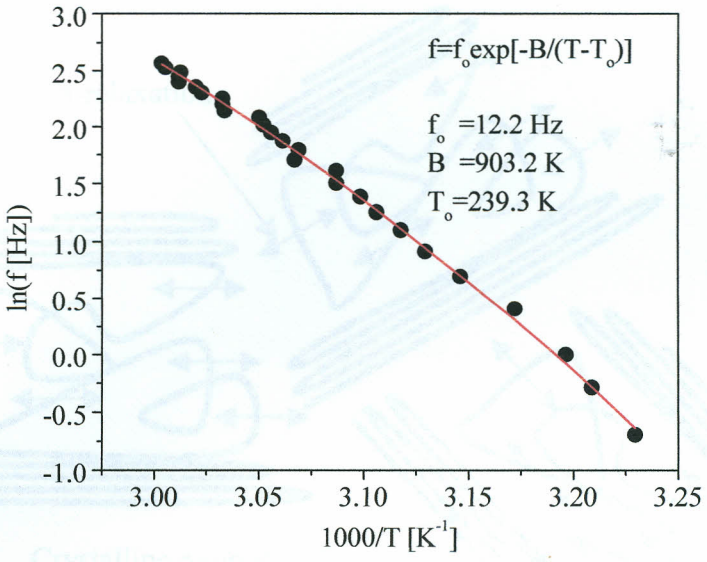

Figure 5.4; The temperature dependence of the relaxation frequency for V0A. The solid curve is a fit according to the VFT law

This observation can be attributed to the fact that HDPE is a semi-crystalline polymer and as a result it has a mixture of regions of different degrees of order which range from completely ordered crystallites to completely amorphous regions. As the temperature is increased the polymer softens and large segmental motions in the amorphous regions become possible. The presence of crystallites however imposes restrictions to large segmental motion of chains since chains are confined to move between crystalline regions. As a result the chains undergo two dimensional chain fluctuations as shown in Figure 5.5.

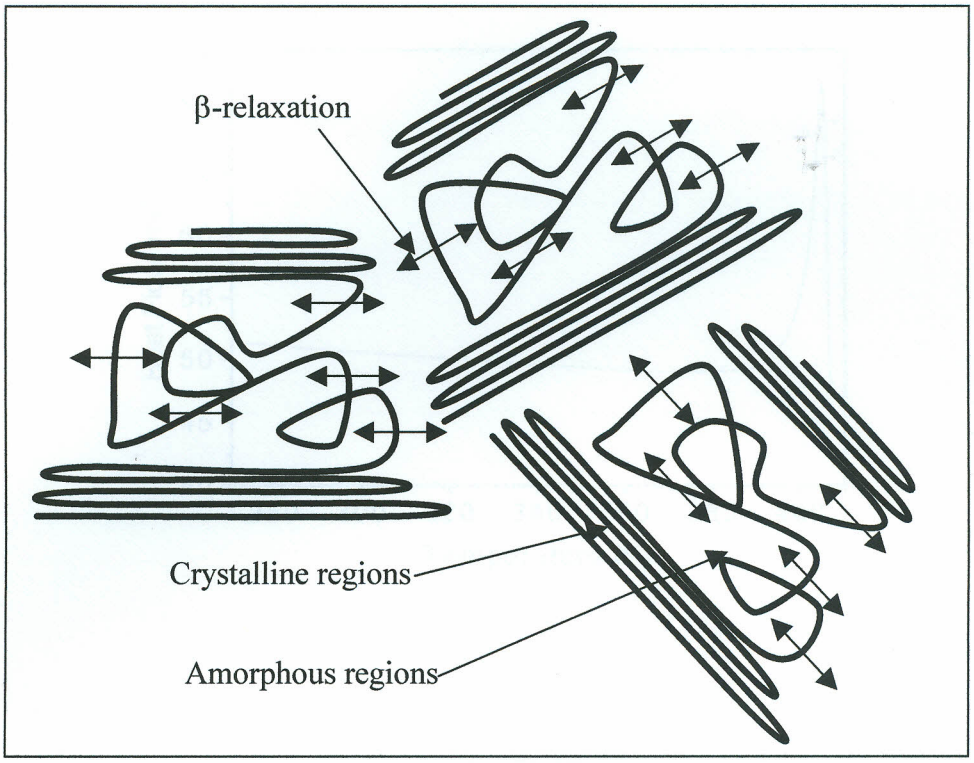

Figure 5.5: Assignment of the observed relaxation process

The presence of only a crystalline melting, T_m peak and absence of a glass transition, T_g peak in the DSC thermogram for V0A, shown in Figure 5.6, agrees with assignment of relaxation process as a 2-dimension chain fluctuation. Primary relaxations have 3-dimensions and also show a T_g peak (Strobl, 1997; Billmeyer, 1984; Sperling, 1992)

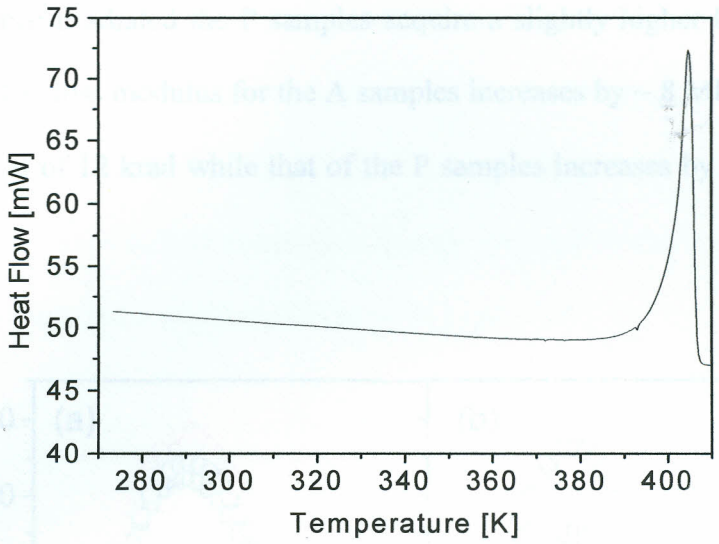

Figure 5.6; DSC thermogram for V0A

The crystalline melting temperature obtained for the DSC thermogram is 405.02 K. This value is close to the value 407.6 K obtained by Macos *et al*, in a DSC study of the morphology of polyethylenes made by Zieglar-Natta catalysts (Macos *et al*, 2001).

The absence of a glass transition, T_g, peak in the DSC thermogram is an indication of the fact that polyethylene is semicrystalline.

5.3 Anisotropy of the Injection Molded Samples

Anisotropy refers to the difference in magnitude of properties observed in different directions. Figure 5.7 shows the intensities of loss modulus E'' versus temperature for samples cut along, A and those cut perpendicular to the melt flow, P. It can be seen that the loss modulus for samples cut along (V0A) is higher than for those cut perpendicular (V0P) to the melt flow directions for the virgin samples. However as the

irradiation dose is increased, the loss modulus for both samples increase. We notice however, that once irradiated the P samples acquire a slightly higher loss modulus than the A samples. The loss modulus for the A samples increases by ~ 8 MPa between a dose of 0 krad and that of 12 krad while that of the P samples increases by ~ 16 MPa for the same range.

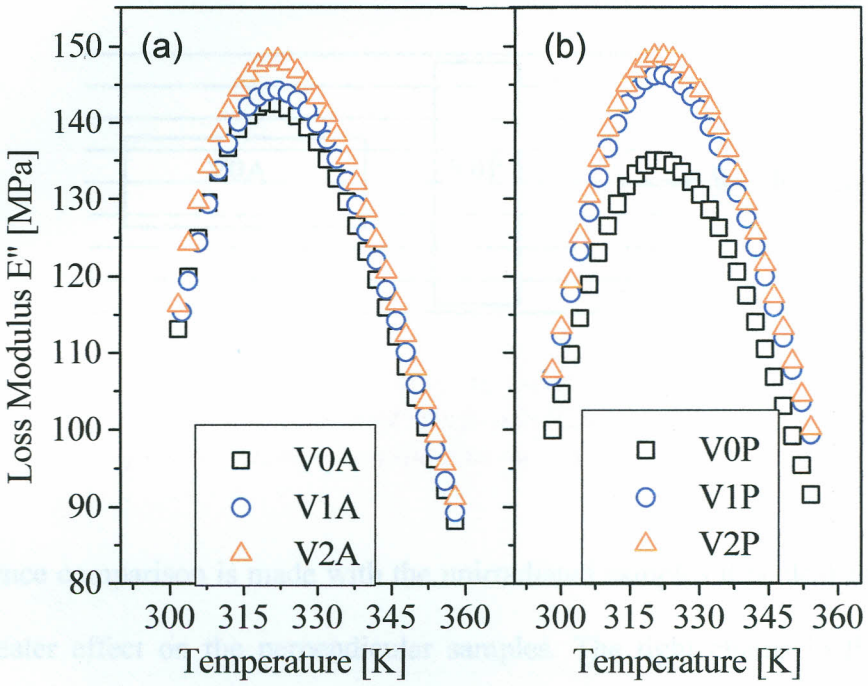

Figure 5.7; Effect of radiation dose on the loss modulus as a function of temperature for VHDPE; (a) samples cut along (b) samples cut perpendicular to the melt flow direction

The above observation can be attributed to the fact that during injection molding molecules move under the influence of pressure, and as a result the chains tend to untangle and orient in the direction of flow, which is radial (Mark et al, 1987). The chains move so rapidly that Brownian motion has no sufficient time to have an appreciable

effect, as such when the sample is cut along (V0A), during clamping the chains are held in such a way that most ends of chains are clamped. The chains will, therefore, oppose any force trying to bend them. On the other hand for the P samples the chains are not clamped but held loosely side by side (V0P). This means that they offer less resistance to bending, and this results in less mechanical energy loss. An illustration of this model of chain orientation and chain alignment is shown in Figure 5.8.

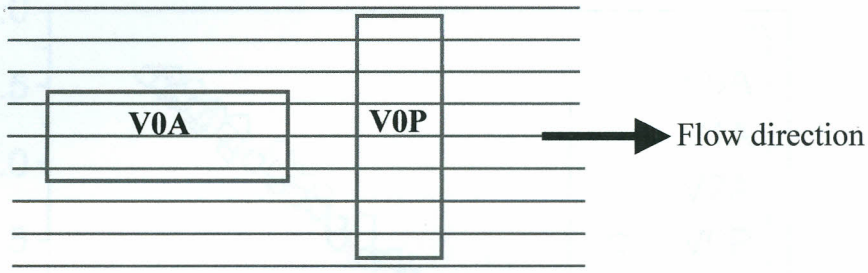

Figure 5.8; An illustration of the possible alignment of chains for Samples cut along and perpendicular to the flow direction. Samples are clamped on the narrow sides

Once comparison is made with the unirradiated samples it is clear that irradiation has a greater effect on the perpendicular samples. The tight chains in the A samples weaken interaction with radiation, while as in the case of P samples interaction is better since the chains are loosely held and also happen to be shorter as compared to those in the A samples, hence the chain respond more when irradiated.

5.4 Effect of Gamma Ray Radiation Dose on the Temperature Dependence of the Relaxation Time

The results in Figure 5.9 indicate that there is an overlap of the activation curves. This is an indication that a gamma ray radiation dose of up to 12 krad, has no effect on the relaxation frequency of the process, which is a large scale motion.

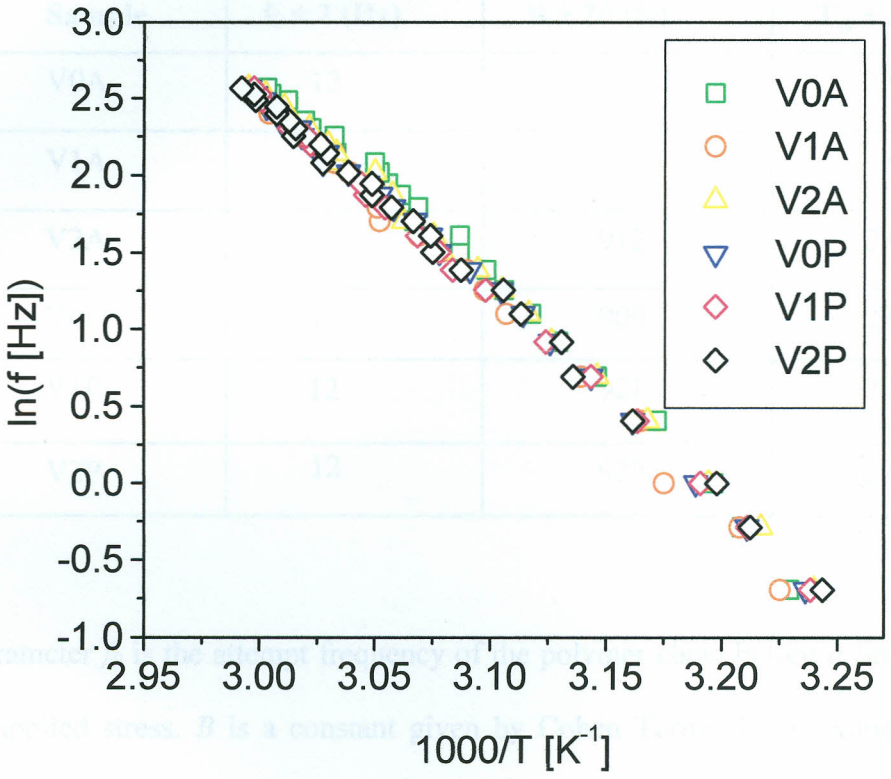

Figure 5.9; Effect of Gamma ray radiation dose on the relaxation frequency as a function of inverse temperature for VHDPE, for samples cut along and perpendicular to the melt flow direction

This fact is further supported by the VFT parameters in Table 5.1, which shows no effect on the attempt frequency of the samples. The value of T_0 is also observed to be unaffected by irradiation of up to 12 krad. It is however possible that at higher doses significant changes may be observed.

Table 5.1; VFT fit parameters for the β - relaxation of the VHDPE

Sample	$f_0 \pm 2$ (Hz)	B ± 20 (K)	$T_0 \pm 2$ (K)
V0A	12	903	239
V1A	12	911	239
V2A	12	912	237
V0P	12	909	237
V1P	12	921	236
V2P	12	920	236

The parameter f_0 is the attempt frequency of the polymer chain before it finally responds to the applied stress. B is a constant given by Cohen Turnbull free volume theory, as explained in section 3.2.5

5.5 Effect of Gamma Ray Radiation Dose on the Melting Temperature of VHDPE

The DSC thermogram in Figure 5.10 shows the heat flow versus temperature for samples irradiated with different doses for the VHDPE. From the results, it is observed that with increasing dose there is no effect observed in the peak shift. This is an

indication of the fact that only very minimal crosslinking effect is achieved, as observed in the loss modulus curves, and as such it results in no effect in the crystalline melting temperature. It is possible that at higher doses some changes could be observed in the crystalline melting temperature.

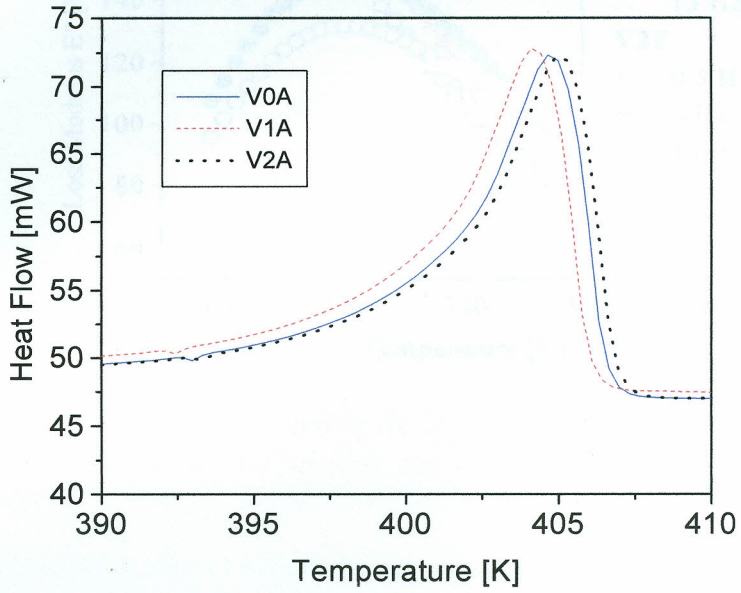

Figure 5.10; Effect of gamma ray radiation dose on the DSC thermograms of VHDPE

5.6 Anisotropy Between Samples Cut Near and Far from the Injection Point

The anisotropy of the samples can be analyzed from the differences in dynamic mechanical behavior between samples cut near the injection point and those cut far away from the injection point. Figure 5.11 shows the intensities of the loss modulus versus temperature for samples cut near and perpendicular to the melt flow direction N, and

those cut far and perpendicular to the melt flow direction F, from the injection point. Clearly the loss modulus for the F samples has a higher intensity than for the N samples.

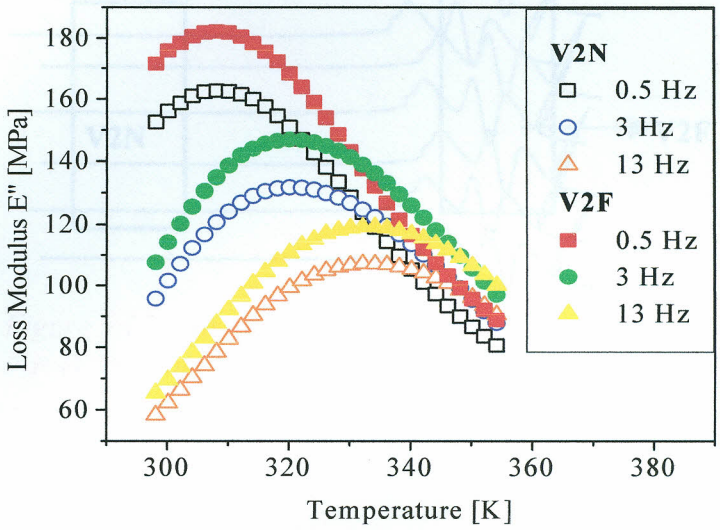

Figure 5.11; Loss modulus as a function of temperature for samples cut near and far from the injection point, For V2F and V2N

The injection molding process introduces anisotropy in the mold disc. During injection molding, the polymer melt is injected under pressure, which in turn aligns the chain with the mold surface. This pressure decreases with increasing distance from the injection point, such that far away from the injection point there is tumbling of the polymer melt. Furthermore the flow of the polymer melt pulls the remainder of the molecules in the direction of flow. This results in formation of the most oriented layers near the injection point. Due to tumbling the outer circumference end up being entangled

(Mark et al, 1987; Morton-Jones, 1989). An illustration of this scenario is as shown in Figure 5.12.

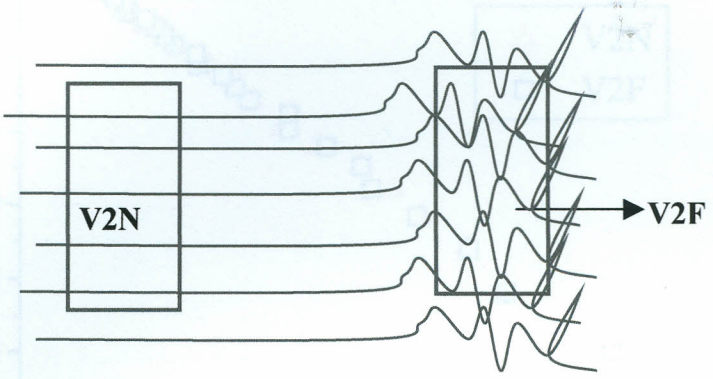

Figure 5.12; Possible chain alignment Near (V2N) and Far (V2F) from the injection point

As a result samples cut far from the injection point have chains with a lower level of order as compared to samples near the injection point. The F samples therefore tend to have natural cross-linking due to entanglement. This opposes separation during bending leading to a high loss modulus. As for the N samples they are highly crystalline with almost no entanglement of chains as such they offer slightly less opposition to bending resulting in less losses.

Figure 5.13 shows the activation plot for the irradiated N and F. The results show an overlap of the relaxation curves. Again this is an indication that any observed changes in the loss modulus curves do not affect the large-scale relaxation. This could mean that gamma ray radiation resulted in small scale cross linking that does not affect large scale motions of the polymer.

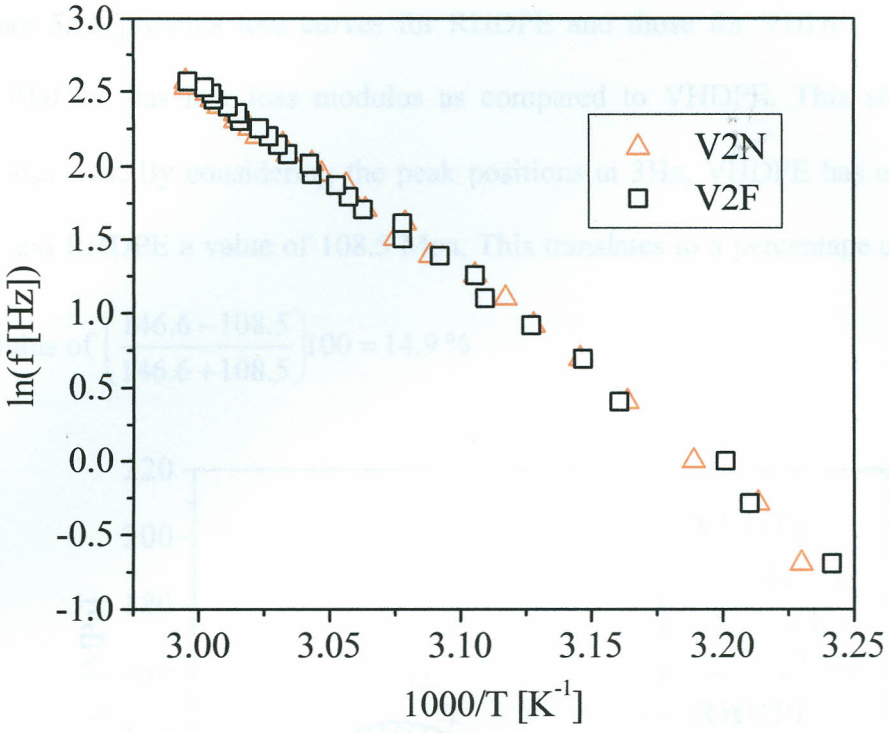

Figure 5.13; The temperature dependence of the relaxation frequency for V2N and V2F

Table 5.2 of the fitting parameters of the relaxation process also indicates that there is no shift in the attempt frequency or T_g parameters of the DMA.

Table 5.2; VFT fit parameters of the β-relaxation of VHDPE

Sample	$f_0 \pm 2$ (Hz)	B ± 20 (K)	$T_0 \pm 2$ (K)
V2N	12	913	237
V2F	12	919	236

5.7 Comparison of the Intensity of the Loss Curves for VHDPE and RHDPE

Figure 5.14 presents loss curves for RHDPE and those for VHDPE. It can be noted that RHDPE has low loss modulus as compared to VHDPE. This shows that RHDPE is less stiff. By considering the peak positions at 3Hz, VHDPE has a value of 146.6 MPa and RHDPE a value of 108.5 Mpa, This translates to a percentage difference in loss modulus of $\left(\frac{146.6-108.5}{146.6+108.5}\right)100 = 14.9\,\%$

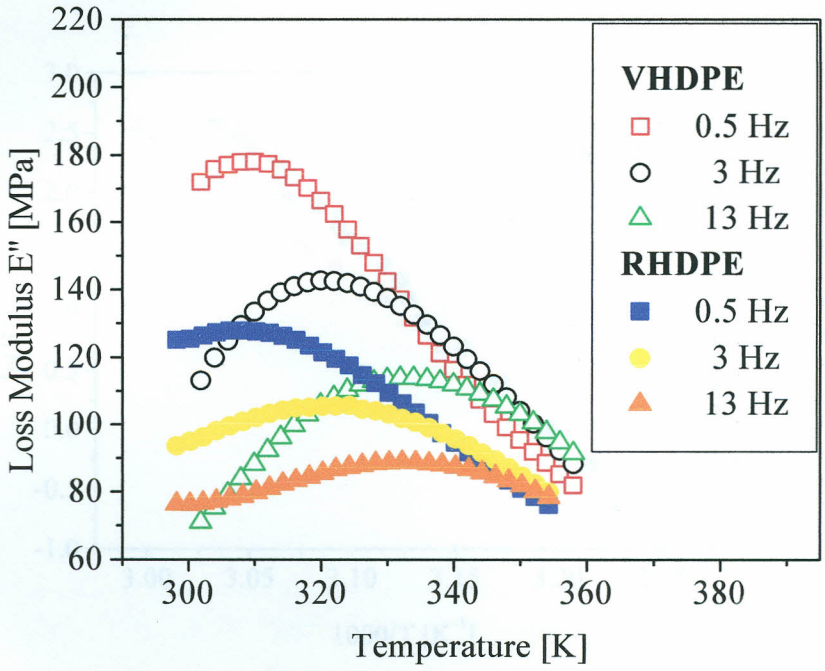

Figure 5.14; Loss modulus as a function of temperature for VHDPE and RHDPE

It is important to note at this point that polymer recycling involves collection of the already used polymer, cleaning, sorting and then characterizing according to material properties. The polymer is then heated until it melts, allowed to cool and finally cut into pellets. These processes seem to have a significant effect of softening the polymer. Furthermore cleaning may not be perfect and the presence of impurities such as paper and

metal foil, may affect how the chains pack. In addition some degradation also, might have occurred during the first lifetime of the recycled polymer. The degradation could result from environmental factors such as, ultra violet light, attack from pollutant gases in urban environments and chemical interaction with liquid content. All this would result in a dispersed (short) chain system. As a result there is a weak interchains interaction that leads to less resistance to chain separation during sample bending, resulting in lesser mechanical energy losses.

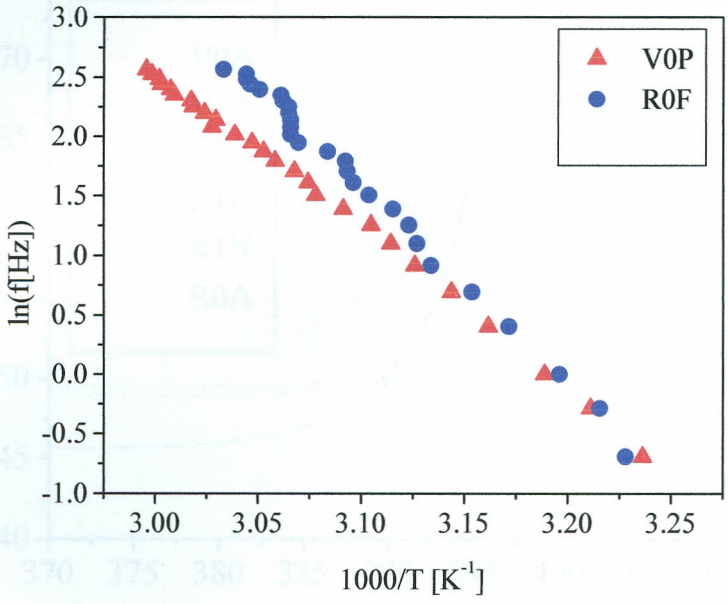

Figure 5.15; A comparison of the relaxation process of VHDPE versus RHDPE

Figure 5.15 shows the mean relaxation process of the VHDPE and RHDPE samples. It can be observed that the relaxation plots for both RHDPE and VHDPE are curves, an indication that both relaxations have a temperature dependence that follows the Vogel Fulcher Tammann (VFT) law (Danch, 2003), already mentioned in section 5.2.

The relaxation frequency of the V0P samples is higher than those of R0F in the high temperature range. This is due to the fact that the R0F samples are softer, in this case the relaxation process becomes faster. The DSC thermograms of Figure 5.16 also further agree with the observation of the relaxation process. We notice that the RHDPE has a lower crystalline melting temperature as compared to VHDPE, an indication that RHDPE is softer.

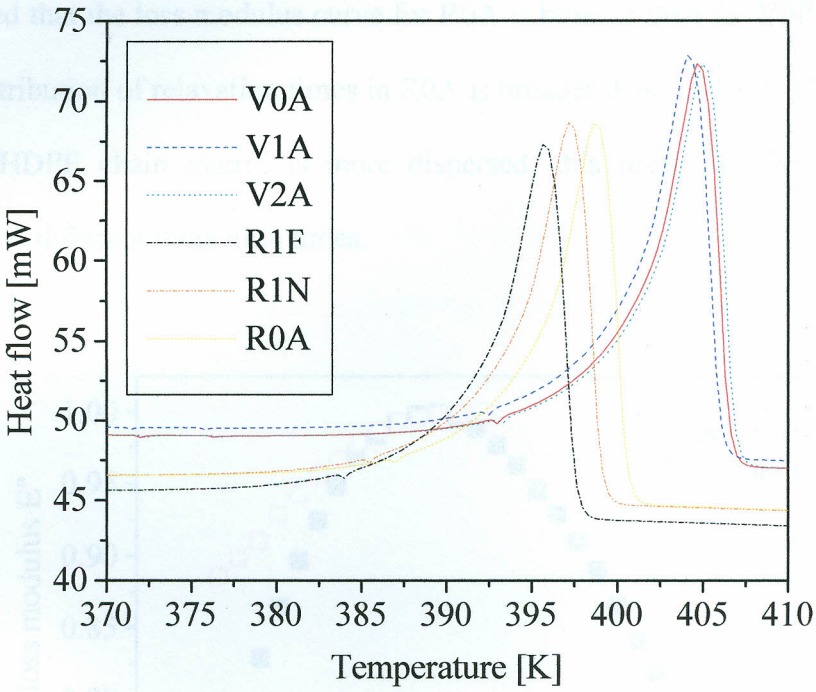

Figure 5.16; A comparison of the DSC thermograms for VHDPE and RHDPE

The fact that the relaxation process becomes faster and the melting temperature decreases with dose intake indicates a softening effect, which could further be taken to mean that significant chain scission occurred. The VFT fit parameters of RHDPE are shown in Table 5.3. There is no shift in the VFT fit parameters.

Table 5.3; VFT fit parameters of the β-relaxation of RHDPE

Sample	$f_0 \pm 2$ (Hz)	B ± 20 (K)	$T_0 \pm 2$ (K)
R1F	12.8	912.8	241.6
R0F	13.6	952.6	243.3

5.7.1 *Normalized Loss Modulus Versus Temperature for V0A and R0A*

Normalized loss modulus curves for V0P and R0A are as shown in Figure 5.17. It can be noted that the loss modulus curve for R0A is broader than for V0P. This indicates that the distribution of relaxation times in R0A is broader than for V0P. This would mean that the RHDPE chain matrix is more dispersed, this results in the various chains responding at different relaxation times.

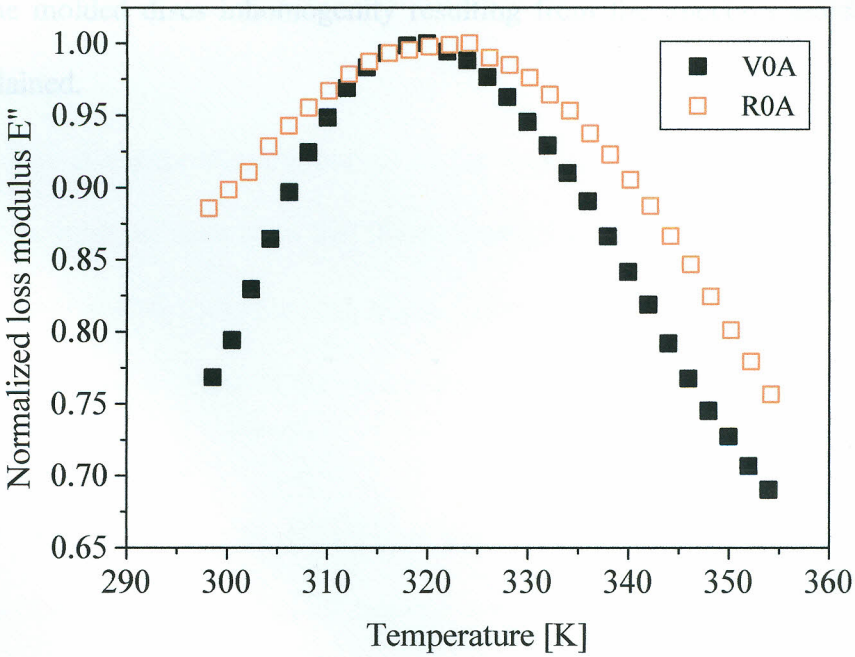

Figure 5.17; A normalized loss modulus as a function of temperature for VHDPE and RHDPE at 3 Hz

The dispersed system could have resulted from degradation, such as photo-degradation that could have occurred during the first lifetime. This could result in chain scission. This observation could also explain why upon irradiation the RHDPE undergoes chain scission resulting in softening. It is possible that the radiation energy encounters an already weakened matrix and application of more energy goes to break the chains further.

5.8 Anisotropy of the RHDPE for Samples Cut Near and Far From the Melt Injection Point

Figure 5.18 presents the results of the loss modulus for samples of RHDPE cut near and far from the melt injection point. It can be noted that for both irradiated and unirradiated RHDPE, intensities for the loss modulus curves are higher for samples cut far from the injection point than for samples cut near the injection point. This anisotropy is due to the molded discs inhomogenity resulting from the injection molding process already explained.

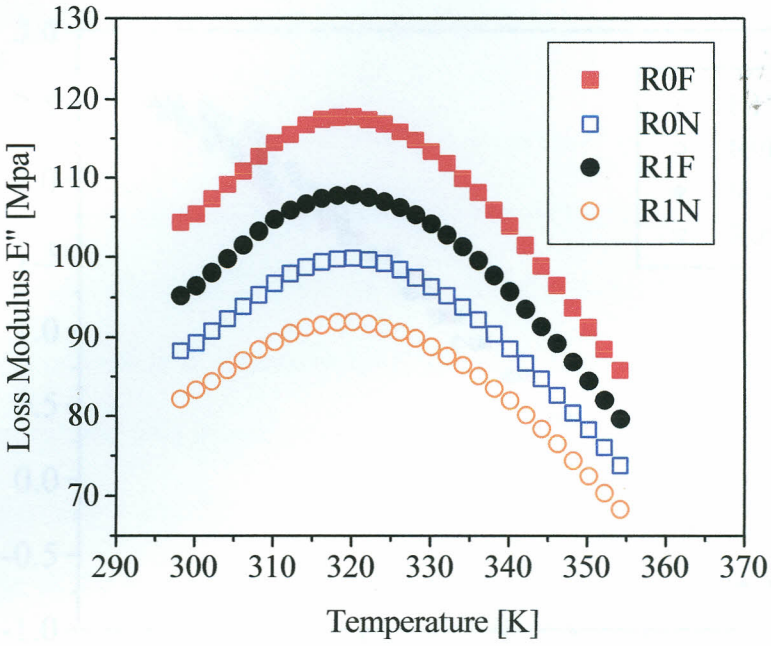

Figure 5.18; Effect of Gamma ray radiation dose on the anisotropy in the RHDPE samples

The loss modulus intensity curves of the irradiated samples is less than for the unirradiated samples, an indication that there is softening of RHDPE once irradiated, this is an indication that chain scission took place. This observation further supports the DSC results that indicate a decrease of the crystalline melting temperature, observed in Figure 5.16.

Activation plots for the RHDPE samples are as shown in Figure 5.19. It is observed that there is an overlap of the relaxation curves. This indicates that insignificant chain scission took place, such that it has no effect on the relaxation frequency of the large scale motion.

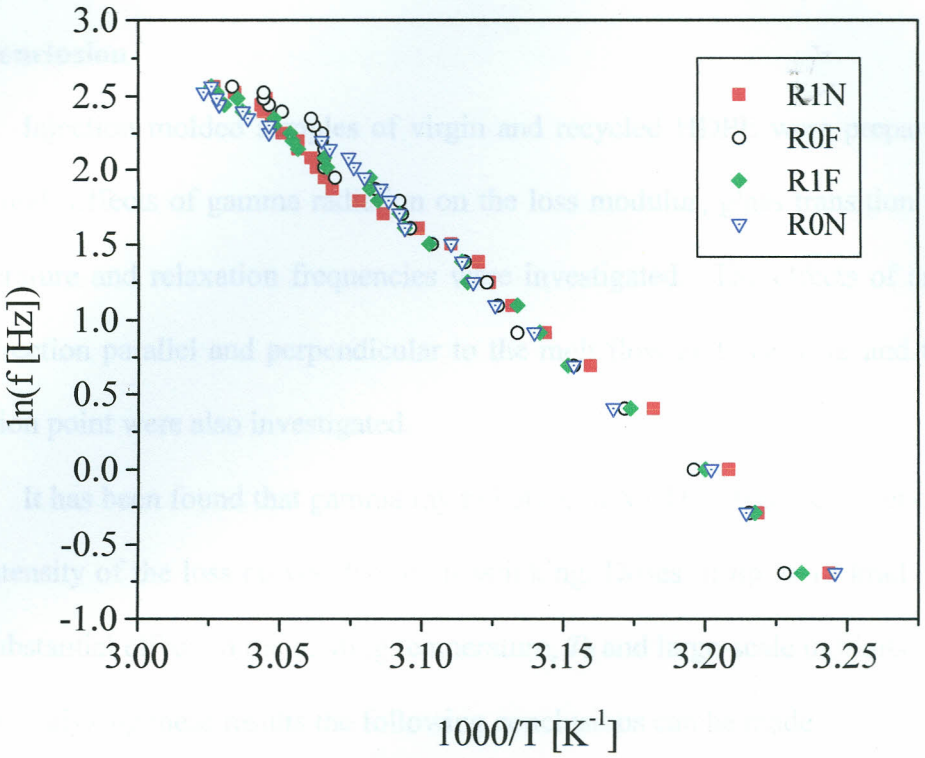

Figure 5.19; Effect of Gamma ray radiation dose on the relaxation frequency of the β process for RHDPE.

CHAPTER 6

CONCLUSIONS AND RECOMMEDATIONS

6.1 Conclusion

Injection molded samples of virgin and recycled HDPE were prepared and then irradiated. Effects of gamma radiation on the loss modulus, glass transition and melting temperature and relaxation frequencies were investigated. The effects of anisotropy in the direction parallel and perpendicular to the melt flow and also near and far from the injection point were also investigated.

It has been found that gamma ray radiation of VHDPE has the effect of increasing the intensity of the loss curves due to crosslinking. Doses of up to 12 krad did not have any substantial effect on the melting temperature, T_0 and large-scale motions of VHDPE.

By analyzing these results the following conclusions can be made.

- DMA investigation of VHDPE and RHDPE in the frequency range 0.5-13 Hz and temperature range 298-355 K reveals one relaxation process. The process is assigned to 2-dimensional chain fluctuations between crystalline regions and obeys VFT law.
- The behavior of virgin and recycled systems differ by approximately 15% owing to the degradation of the recycled system; this is vital from the commercial and industrial point of view because it is possible to use a recycled material, which results in a positive environmental impact. This knowledge enables one to select the recycled material for use in the appropriate areas, which require less energy dissipations.

- Irradiation increases the intensity of the loss modulus curves with increasing dose for VHDPE. This increase can be said to result from polymer chains forming crosslinks or from an increase in the order within the samples. However all the literature studied points to the only possibility being the formation of crosslink, in this case then the crosslinks result in formation of networks. This decreases the freedom of movement of the chains hence increasing the loss modulus as is observed in the results. The crosslinking is however only on a small scale and hence has no effect on the large-scale motions.
- An increase in the loss modulus can also mean an improvement in the impact strength of the material. According to (Bailey, 1981), materials with a high loss modulus incase of an impact are able to dissipate the energy at the point of impact instead of a situation whereby large stresses are created and fracture follows as a result.
- A comparison of the intensities of the loss modulus for samples cut near and those cut far away from the injection point, also those cut along and those cut perpendicular to the melt flow direction, indicate anisotropy in the injection molded samples.
- For the doses of up to 12 krad no substantial changes in the glass transition temperature and the melting temperature of VHDPE was observed. However, irradiation of RHDPE resulted in a decrease of the melting temperature. This is an indication that upon irradiation chain scission took place resulting in softening of the polymer.

From the above conclusions it is evident that gamma ray radiation improves the mechanical properties of HDPE for specific uses. Depending on the area of application, one may need a material with a high loss modulus or one with a low loss modulus. In situations where a polymeric material will be subject to cyclic deformation, high loss modulus would lead to evolution of considerable heat which would contribute to rapid degradation and wear. Thus a material with a low loss modulus would help minimize energy dissipation, and hence the degradation and wear. In other situations the aim is to prevent transmission of vibrations, and in such a situation a material with a high loss modulus would dissipate considerable vibrational energy as heat instead of transmitting it. Dose suitable for desired uses could be selected according to the mechanical property to be modified.

6.2 Recommendations for Further Work

It would be appropriate to use supplementary measurement techniques like the scanning electron microscopy, (SEM), attenuated total reflection (ATR) infrared, or X-ray diffractometry to study the structure of the samples in order to be able to give a more accurate explanation of the molecular dynamics of the irradiated samples.

It would also be necessary to carry out similar studies using higher doses to determine the dose at which the melting temperature of VHDPE can be raised, since this happens to be a major drawback in application of polyethylene. In addition it may be necessary to carry out similar studies using higher doses of gamma radiation on RHDPE as this would shed more light on doses that would give optimum mechanical properties.

REFRENCES

Albano, C., Perera, R., Silva, P. and Sanchez, Y. (2003). Characterization of gamma irradiated PEs using ESR, FTIR, and DSC techniques. *Journal of Polymer Bulletin* 51: P 135 – 142.

Bailey, R. T. (1981). *Molecular motions in high polymers.* Oxford University Press, inc., New York.

Banerjee, S., Sinha, N.K., Gayathri, N., Ponraju, D., Dash, S., Tyagi, A.K. and Raj, B. (2007). Detecting onset of chain scission and crosslinking of gamma irradiated elastomer surfaces using frictional force microscopy. *Journal of Physics D: Applied Physics* 40: P 834 –839.

Billmer, W.F Jr. (1984). *Textbook of polymer science.* John Wiley and Sons, Singapore.

Bodor, G. (1991). *Structural investigation of polymers*. Ellis Horwood Limited, New York

Borgstorm, A., Kolman, L., Ledger, R. and Malik, M. (1998). Mechanical properties of processed ultra high molecular weight polyethylene. Final project, Bioengineering Laboratory 210.

Bovey, F. A. and Winslow, F. H. (1979). *Macromolecules an introduction to polymer science*. Academic press, Inc., San Diego.

Burton, Kirby, S. and Magee. (1960). *Comparative effects of radiation. John Wiley and Sons, New York.*

Cheng, S. and Kerluke, D.R. (2003). Radiation processing for modification of polymers. http://www. iba-worldwide com/Pdf % files / Polymer % 20 paper Pdf.

Cohen, M.H. and Turnbul D. (1954). *Journal Phys. Chem* 31: P 116

Colo, M.S., Hedman, K. and Rudolph, S.B. (1997). Rheological instrumentation for characterization of polymers. http://www. ats rheosystems.com/sni/downloads/ANTEC-paper.pdf.

Considine, D.M. (1974). *Chemical and process technology encyclopedia.* McGraw-Hill, Inc. Newyork.

Cowle, J.M. (1991). *Polymers: Chemistry and Physics of modern materials.* Blackie Academic and Professional, London.

Crawford, R.J. (1998). *Plastic engineering*. Butterworth - Heinmann

Danch, A. (2003). On the influence of supermolecular structure on structural relaxation in the glass transition zone. *Journal of Fibres and Textiles in Eastern Europe* 11: P 128-131

Doolittle, A.K. and Doolittle, D.B. (1957). *Journal of Applied Physics* 28: P901

Ehmann, W.D and Vance, D.E. (1991) *Radiochemistry and nuclear methods of analysis.* John Wiley and Sons, New York.

EL-Naggar, A.M, Zohdy, M.H, Hassan, M.S and Khalil, E.M. (2003). Antimicrobial protection of cotton/polyester fabrics by radiation and thermal treatments. I. effects of ZnO formulation on the mechanical and dyeing properties. *Journal of Applied Polymer Science* 88: P 1129-1137.

EL-Salmawi, K.M, Abu Zaid, M.M, Ibraheim, S.M, EL-Naggar, A.M and Zahran A.H. (2003). *Sorption of dye wastes by poly (Vinyl alcohol), (PVA). Journal of Jolymer Science* 89: P 394-354.

Evora, M.C., Machado, L.D.B., Lourenco, V.L., Goncalenz, O.L., Wiebeck and de Andrade e Silva. (2002). Thermal analysis of ionizing radiation effects on Recycled poyamide-6. *Journal of Thermal Analysis and Calorimetry* 67: P 327 – 333.

Flocke H.A. (1962). *Kolloid – Z . Z polymer.* 180: P 188.

Fried J.R. (1995). *Polymer science and technology.* Prentice Hall, Upper Saddle River.

Gawish, S.M, Kantouch, A, EL-Naggar and A.M, Mosleh S. (1995). Gamma preirradiation and grafting of 2N-morpholino ethyl methacrylate onto polypropylene fabric. *Journal of Applied Polymer Science* 57: P 45-53.

Hay, N. J. (1995) The physical ageing of amorphous and crystalline polymers. *Journal of Pure and Applied Chemistry.* 67: P 1855-1858

http://www.eng Utah.edu/~nairn/classes/mse/-5473/mechanical. Pdf

Ian, M C. (1996) *Introduction to synthetic polymers*. Oxford University Press, New York.

International Commission on Radiation Units and Measurements (ICRU report). (1970). *Radiation dosimetry.* ICRU Publication, Washington D.C.

James, E T. (1986). *Atoms, radiation and radiation protection.* Pergamon Press Inc., New York.

Kaufman, L., Li, J., Plesco, A. and Rogers, J. (1998). Effects of gamma radiation sterilizarion on UHMWPE. B E 210 Final project.

Koizumi, H., Fujimura, A. and Ichikawa, T. (2004). Crosslinking of piezoelectric polymers by ionizing radiation. *Japanese Journal of Applied Physics* 43: P 347 – 348.

Lee, J. Choi, H. W., Nho, Y.C and Suh, D. H. (2003). Gamma ray irradiation effect of polyethylene on Dimaleimides as a class of new multifunctional monomers. *Journal of Polymer Science,* 88: P 2339-2345.

Macos, L. D, Veroni, V. B, Romeu, A. R. and Eloisa, B. M. (2001). Morphology and thermal properties of polyethylenes made by metallocene and Zieglar –Natta catalysts. *Journal of Material Science Innovations,* 4: P 82-88.

Maggi, L., Segale, L., Machiste, E.O., Faucitano, A., Buttafava, A. and Conte, U. (2004). Polymers-gamma ray interaction. Effects of gamma irradiation on modified release drugs delivery system for oral administration. *International Journal of Pharmaceutics* 269: P 343 –351.

Mano, J. F. (2001). Co-operativity in the crystalline α-relaxation of polyethylene. *Journal of Macromolecules,* 34: P 8825-8826.

Mark, Bikales, Overberger and Menges. (1984). *Encyclopedia of polymer science and engineering*, 4. John Wiley and Sons, New York.

Mark, Bikales, Overberger and Menges. (1986). *Encyclopedia of polymer science and engineering*, 4. John Wiley and Sons, New York.

Mark, Bikales, Overberger and Menges. (1987). *Encyclopedia of polymer science and engineering*, 4. John Wiley and Sons, New York.

Mark, Bikales, Overberger and Menges. (1988). *Encyclopedia of polymer science and engineering*. 13. John Wiley and Sons, New York.

Mansour, S.A. (2001). Effects of gamma radiation on the mechanical and relaxation behavior of high and low density polyethylene. *Egypt Journal Sol.* 24

McCrum, N.G., Buckley, C.P. and Bucknall, C.B. (1997). *Principles of polymer engineering.* Oxford science publications, New York.

McCrum, N.G., Read B.E. and William, G. (1967). *Anaelastic and dielectric effects in polymeric solids.*

Messick, J. (2003). Electron beam processing of plastics: an alternative to chemical additives. http://www.E-BEAMSERVICES.COM/../BEAM_SPE_ANTEC.HTM

Morton-Jones, D.H. (1989). *Polymer processing.* Chapman and Hall Ltd, New York.

Mukherjee, A.K. and Gupta, B.D. (1985). Radiation-induced graft co polymerization of methacrylic acid onto polypropylene fibers VI. dyeing behavior. *Journal of Applied Science* 30: P 4455-4466.

Nho, Y.C. and Park, K.R. (2002). Preparation and properties of PVA/PVP hydrogels containing chitosan by radiation. *Journal of Applied Polymer Science* 85: P 1787-1794.

Powel, P.C. and Housz, A,J.I. (1998). *Engineering with polymers.* Stanley thornes publishers.

Reyes, J., Albano, C., Davidson, E., Poleo, R., Gonzalez, J., Ichazo, M. and Chipara, M. (2000) Effects of gamma irradiation on Polypropylene + High density Polyethylene and Polypropylene + High Density Polyethylene + Wood flour. *Journal of material research Innovations* 4: P 294 - 300.

Sayeda, M I. (2003). Synthetic absorbent for dyestuffs based on gamma crosslinked Poly (Vinyl alcohol (PVA). *Journal of Applied Polymer Science* 89: P 349 - 354.

Seguchi, T., Yagi, T., Ishikawa, S. and Sano Y. (2002). New material synthesis by radiation processing at high temperature-polymer modification with improved irradiation technology. *Journal of Radiation Physics and Technology* 63: P 35 - 40.

Sepe, P.M. (1992). Dynamic and mechanical analysis. *Journal of advanced materials and processes*: P 32-34

Sperling, L.H. (1992). *Introduction to physical polymer science* John Wiley and Sons, New York.

Stevens, P. M. (1990). *Polymer chemistry an introduction.* John Wiley and Sons, New York.

Strobl, G. (1997). *The physics of polymers, concepts for understanding their structure and behavior.* Springer Verlag, Berlin Heidenberg.

Usanmaz, A., Eser, O. and Dogan, A. (2001). Thermal and dynamic mechanical properties of gamma ray cured poly (methyl methacrylate) used as a dental base material. *Journal of Applied polymer Science* 81: P 1291 – 1296.

Valenza, A. and Spadaro, G. (1993). Polymer engineering and science. *Journal of Applied Polymer Science* 33: P 13.

Vogel, A. (1921). *Physik.* 22: P 645.

Wang, Q., Gao, J., Wang, R. and Hua Z. (2001). Mechanical and rheological properties of HDPE (Graphite composite with enhanced thermal conductivity), *Journal of polymer composites* 22: P 97.

Ward, I. M. and Hadley D.W. (1993). *An introduction to the mechanical properties of solid polymers.* John Wiley and Sons Ltd, New York

Williams, J. G. (1980). *Stress analysis of polymers.* Ellis Horwood Limited, England.

Zainuddin, Albinska, J., Ulanski, P. and Rosiak J.M. (2002). Radiation-induced degradation and crosslinking of poly(ethylene oxide) in solid state. *Journal of radio analytical and nuclear chemistry* 253: P 339 – 344.

Zhen, J.S. (2001). The effect of chain flexibility and chain mobility on radiation crosslinking of polymers. *Journal of Radiation Physics and Chemistry* 60: P 445 _ 451.